Quantum Entanglement of One-Dimensional Spinless Fermions

A Thesis Presented

by

Emanuel Casiano-Diaz

to

The Faculty of the Graduate College

of

The University of Vermont

In Partial Fullfillment of the Requirements
for the Degree of Master of Science
Specializing in Physics

April 30th, 2018 or before (Writing Complete)

Defense Date: May 30th, 2018
Thesis Examination Commitee:

Adrian Del Maestro, Ph.D, Advisor
Dennis Clougherty, Ph.D
Christopher Danforth, Ph.D, Chairperson
Cynthia J. Forehand, Ph.D, Dean of the Graduate College

Abstract

Quantum Entanglement.....

Acknowledgements

I want to thank .....

Contents

Chapter 1

Introduction

PARAGRAPH DESCRIBING WHAT WILL BE DONE IN THE SECTIONS OF THIS CHAPTER

1.1 Quantifying Entanglement

1.1.1 Shannon Entropy

1.1.2 Von Neumann Entropy

1.1.3 Rényi Entropy

1.2 Measurement on a microscopic model

1.2.1 The tV model

1.3 Types of bipartitions

1.3.1 Entanglement between spatial subregions

1.3.2 Entanglement between subsets of particles

1.3.3 Operational Entanglement

Chapter 2

Particle Partition Entanglement in the tV Model

2.1 Abstract

We investigate the scaling of the Rényi entanglement entropies for a particle bipartition of interacting spinless fermions in one spatial dimension. In the Tomonaga-Luttinger liquid regime, we calculate the second Rényi entanglement entropy and show that the leading order finite-size scaling is equal to a universal logarithm of the system size plus a non-universal constant. Higher-order corrections decay as power-laws in the system size with exponents that depend only on the Luttinger parameter. We confirm the universality of our results by investigating the one dimensional $t-V$ model of interacting spinless fermions via exact-diagonalization techniques. The resulting sensitivity of the particle partition entanglement to boundary conditions and statistics supports its utility as a probe of quantum liquids.

2.2 Introduction

Identical particles are fundamentally indistinguishable in quantum mechanics, unlike their classical counterparts that can always be discriminated due to an infinite set of observable properties. While this indistinguishability allows for the power provided by the second quantization formalism, it can also lead to ambiguity [Zanardi, 2001, Shi, 2003, Shi, 2004] when considering another defining property of composite quantum systems: entanglement. A pure state representing N quantum particles $|\Psi\rangle \in \mathcal{H}$ in Hilbert space $\mathcal{H}$ is said to be bipartite entangled if it cannot be written in a simple tensor product form $|\Psi\rangle \neq |\Psi_A\rangle \otimes |\Psi_B\rangle$ where A and B are vector spaces with $|\Psi_A\rangle \in A$ and $|\Psi_B\rangle \in B$ such that $A \otimes B = \mathcal{H}$. Conventionally, A and B correspond to a set of distinguishable single-particle modes whose occupation numbers are physical observables, i.e., spatial or momentum modes. However, for indistinguishable itinerant particles, there is no natural tensor product decomposition into single-particle modes due to the symmetrization or anti-symmetrization of the wavefunction with respect to the interchange of first quantized particle coordinates for bosons and fermions, respectively. Thus, the *mode entanglement* may depend on the choice of single-particle modes, leading to questions as to which (if any) are preferred and moreover, if these quantum correlations are even physically meaning-

ful [Ghirardi and Marinatto, 2004, Barnum et al., 2004, Dunningham et al., 2005, Wiseman et al., 2003, Wiseman and Vaccaro, 2003a, Benatti et al., 2012, Balachandran et al., 2013 Dalton et al., 2017]. For example, even in the absence of interactions, a system of N free itinerant bosons [Simon, 2002, Ding and Yang, 2009] or fermions [Schliemann et al., 2001, Zanardi, 2002, Zanardi and Wang, 2002] is always entangled under a spatial bipartition as a result of all allowed states being normalized linear combinations of Slater determinants or permanents.

Insights into these issues can be gained by considering the N-body wavefunction in first quantized form where a bipartition can be made in terms of identical particle labels. The resulting *n-particle partition entanglement* is a measure of quantum correlations between the subsets of n and $N - n$ particles. As individual (or groups of) identical particles are not operationally distinguishable, there have been claims that this type of entanglement is not useful as a resource for quantum information processing [Ghirardi and Marinatto, 2004, Tichy et al., 2011, Balachandran et al., 2013]. However, schemes have been recently proposed to transfer it to experimentally addressable modes [Killoran et al., 2014]. In a foundational series of papers, Haque *et al.* explored the particle partition entanglement in fractional quantum hall [Zozulya et al., 2007, Haque et al., 2007] and itinerant bosonic, fermionic and anyonic lattice gases in one spatial dimension [Zozulya et al., 2008, Haque et al., 2009]. This type of particle partition entanglement has since been investigated in other one dimensional systems including the fermionic Calogero-Sutherland [Katsura and Hatsuda, 2007], anyonic hard-core [Santachiara et al., 2007] and bosonic Lieb-Liniger [Herdman et al., 2014, Herdman and Del Maestro, 2015] models as well as rotating bose and fermi gases in two dimensions [Liu and Fan, 2010]. In analogy to the universal finite size scaling behavior of the entanglement entropy of one dimensional quantum gases under a spatial mode bipartition [Calabrese and Cardy, 2004, Calabrese et al., 2011a, Calabrese et al., 2011b], a leading order scaling form for the particle partition entanglement entropy S supported by exact diagonalization on small lattice models was proposed in Ref. [Zozulya et al., 2008] which is linear in the subsystem size n and logarithmic in the system size N: $S \sim n \ln N$.

Motivated by this empirical prediction, in this paper, we investigate the particle partition entanglement for itinerant interacting spinless fermions in one spatial dimension. For Galilean invariant systems in the spatial continuum, we confirm the scaling form proposed in Ref. [Zozulya et al., 2008] within the Tomonaga-Luttinger liquid framework [Tomonaga, 1951, Haldane, 1981] and determine how the leading order power-law corrections to the asymptotic scaling depend on the strength of the interactions between particles for $n = 1$. By exploiting symmetries of the n-particle reduced density matrix, we are able to measure the particle entanglement entropy in the one dimensional fermionic $t - V$ model for systems composed of up to $M = 28$ lattice sites at half filling, allowing us to confirm our predictions from continuum field theory.

The rest of this paper is organized as follows. We introduce a quantitative measure of entanglement, the Rényi entanglement entropy and discuss some known results for interacting spinless fermions. We then derive the 1-particle entanglement entropy in the low energy limit and compare with exact diagonalization results on a lattice. We conclude with a discussion of the role of boundary conditions, degeneracy and implications for future studies of models with generalized statistics. All numerical data and code necessary to reproduce the results and figures in this

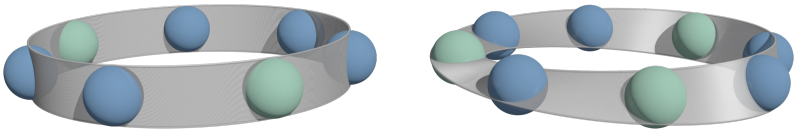

periodic: $N = 7,\ n = 2$ anti-periodic: $N = 8,\ n = 3$

Figure 2.1: A schematic of $N = 7$ fermions in one spatial dimension subject to periodic boundary conditions under a n-particle partition with $n = 2$ (left) and anti-periodic boundary conditions with $N = 8$ and $n = 3$ (right). All fermions are identical, while the partitions A and B are distinguished via their first quantized labels.

paper can be found in Ref. [rep,].

2.3 Particle Partition Entanglement

The entanglement of the pure state $\big|\Psi\big\rangle$ under a general bipartition into A and B can be quantified via the Rényi entanglement entropy:

$$S_\alpha\left[\rho_A\right] \equiv \frac{1}{1-\alpha}\ln\left(\mathrm{Tr}\rho_A^\alpha\right), \tag{2.1}$$

where α is the Rényi index and ρ_A is the reduced density matrix obtained by tracing out all degrees of freedom in B

$$\rho_A \equiv \mathrm{Tr}_B\left|\Psi\right\rangle\!\left\langle\Psi\right|. \tag{2.2}$$

For $\alpha = 1$ the Rényi entropy is equivalent to the von Neumann entropy: $-\mathrm{Tr}\ \rho_A \ln \rho_A$.

While it is common for A and B to be defined by some set of observable modes, for a many-body system consisting of N itinerant particles they can refer to subsystems of particles. As depicted in Fig. A.4, such a bipartition of indistinguishable particles (in this case spinless fermions) is completely specified by the number of particles in the subsystem, n. The entanglement entropy under a particle bipartition is then a function of the familiar n-body reduced density matrix ρ_n, (n-RDM) defined in first quantized notation in one spatial dimension as:

$$\rho_n \equiv \int dx_{n+1}\cdots\int dx_N\,\langle x_{n+1}\cdots x_N|\Psi\rangle\,\langle\Psi|x_{n+1}\cdots x_N\rangle \tag{2.3}$$

where we have taken the normalization $\mathrm{Tr}\rho_n = 1$. From this form, it is clear that the particle partition Rényi entropies $S_\alpha[\rho_n] \equiv S_\alpha(n)$ only vanish when the N-body ground state $\big|\Psi\big\rangle$ can be written as a general tensor product state in first quantized notation. This immediately implies that $S_\alpha(n) = 0$ when all particles are condensed into a single mode, and thus the particle partition entanglement of the non-interacting Bose gas is identically zero, in contrast to non-zero results for its spatial mode entanglement [Simon, 2002, Ding and Yang, 2009]. This is not the case for many-fermion systems, which always have non-zero particle entanglement, even in the absence of interactions [Zanardi, 2002]. Particle entanglement entropy is sensitive to both interactions and statistics, and as ρ_n is free of any length scale,

it can capture non-local effects making it complimentary to the more conventionally studied spatial mode entanglement entropy.

As described in the introduction, Zozulya et al. [Zozulya et al., 2008] first proposed a "standard" finite-size scaling form for the particle entanglement entropy of fermions:

$$S(n,N) = \ln \binom{N}{n} + a + \mathcal{O}\left(\frac{1}{N^\gamma}\right) \tag{2.4}$$

where a and γ are non-universal dimensionless numbers that can depend on n. These coefficients are known for the case of non-interacting fermions where $a = 0$ [Haque et al., 2009] and for the Laughlin state with filling fraction ν: $a = -n \ln \nu$, $\gamma = 2$ when $n \ll N$ [Zozulya et al., 2007].

Recently, a general scaling form like Eq. (2.4) was investigated for a system of interacting bosons in the spatial continuum with $n = 1$ [Herdman and Del Maestro, 2015] where it was found that the pre-factor of the leading order logarithm is non-universal, depending on the interaction strength. In this paper, we apply extensions of these methods to interacting Galilean invariant one dimensional fermions and are able to systematically derive Eq. (2.4) while presenting results for both a and γ as a function of the interaction strength.

2.4 One-particle entanglement in fermionic Tomonaga-Luttinger liquids

We are interested in the asymptotic finite size scaling of the entanglement entropy (EE) as defined in Eq. (2.1) which can be investigated for any Rényi index α. Here we focus on the special case of $\alpha = 2$ as (i) the calculation will turn out to be analytically tractable and (ii) as it can be related to the expectation value of a local observable, it has proved to be the most direct numerical [Hastings et al., 2010, Grover, 2013, McMinis and Tubman, 2013, Drut and Porter, 2015] and even experimental [Islam et al., 2015, Melko et al., 2016] route to its measurement. We begin by considering a system of N one-dimensional interacting spinless fermions with density $\rho_0 = N/L$ (where L is the length of the system) whose low energy properties can be described in terms of the universal quantum hydrodynamics of Tomonaga-Luttinger liquid (TLL) theory [Tomonaga, 1951, Haldane, 1981]. Within this framework, at zero temperature in the thermodynamic limit, any n-body reduced density matrix can in principle be computed [Giamarchi, 2004] and in particular for $n = 1$ [Dzyaloshinskii and Larkin, 1974]

$$\rho_1(x,x') = \frac{\sin(\pi\rho_0|x-x'|)}{\pi\rho_0 L|x-x'|(1+|x-x'|^2\Lambda^2)^{(K+K^{-1}-2)/4}}, \tag{2.5}$$

where $\mathrm{Tr}\,\rho_1 = 1$ and both the ultraviolet (inverse short-distance) cutoff Λ and TLL parameter K depend on the microscopic details of the interaction between particles. Specifically, K characterizes the nature of the interaction, where $0 < K < 1$ ($K > 1$) corresponds to repulsive (attractive) interactions with free fermions having $K = 1$. For ease of notation, we will replace the non-negative K-dependent exponent in Eq. (2.5) with $g \equiv (K + K^{-1} - 2)/4$.

The one-particle partition second Rényi entanglement entropy can be computed by using ρ_1 in Eq. (2.1)

$$\begin{aligned} S_2(n=1) = -\ln\left(\mathrm{Tr}\left[\rho_1^2\right]\right) &= -\ln\left(\int_{-L/2}^{L/2} dx \int_{-L/2}^{L/2} dx' \rho_1(x,x')\,\rho_1(x',x)\right) \\ &= \ln(N) - \ln(f(N,g,\Lambda/\rho_0)), \end{aligned} \tag{2.6}$$

where we have used translational invariance of the system and

$$\begin{aligned} f(N,g,\Lambda/\rho_0) = &\int_0^\infty dy \frac{2\sin^2(\pi y)}{\pi^2 y^2 (1+y^2\Lambda^2/\rho_0^2)^{2g}} \\ &- \int_{N/2}^\infty dy \frac{2\sin^2(\pi y)}{\pi^2 y^2 (1+y^2\Lambda^2/\rho_0^2)^{2g}}. \end{aligned} \tag{2.7}$$

The first integral can be evaluated exactly in terms of special functions:

$$\begin{aligned} A(g,\Lambda/\rho_0) = &\int_0^\infty dy \frac{2\sin^2(\pi y)}{\pi^2 y^2 (1+y^2\Lambda^2/\rho_0^2)^{2g}} \\ = &\frac{\pi^{4g+\frac{1}{2}}\rho_0^{4g}\sec(2\pi g)\,{}_1F_2\left(2g;2g+1,2g+\frac{3}{2};\pi^2\Lambda^{-2}\rho_0^2\right)}{2\Lambda^{4g}\Gamma(2g+1)\Gamma(2g+\frac{3}{2})} \\ &+ \frac{\Lambda\Gamma\left(2g+\frac{1}{2}\right)\left[{}_1F_2\left(-\frac{1}{2};\frac{1}{2},\frac{1}{2}-2g;\pi^2\Lambda^{-2}\rho_0^2\right)-1\right]}{\pi^{3/2}\rho_0\Gamma(2g)}. \end{aligned} \tag{2.8}$$

where ${}_1F_2(q;c,d;z)$ is the generalized hypergeometric and $\Gamma(z)$ the Gamma function. The leading order N dependence of the second integral in Eq. (2.7) can be extracted by replacing the highly oscillating periodic function $\sin^2(\pi y)$, in the large N limit, by its average over one period, i.e., $\sin^2(\pi y) \approx 1/2$ and expanding the rest of the integrand for large y. We find

$$f(N,g,\Lambda/\rho_0) \simeq A(g,\Lambda/\rho_0) - \frac{2^{4g+1}}{\pi^2(4g+1)(\Lambda/\rho_0)^{4g}}\frac{1}{N^{4g+1}} \tag{2.9}$$

and thus the second Rényi EE for $n=1$ has the asymptotic form

$$S_2(n=1) = \ln(N) - \ln\left[A(g,\Lambda/\rho_0)\right] + \frac{b(g,\Lambda/\rho_0)}{N^{4g+1}} + \mathcal{O}\left(\frac{1}{N^{4g+2}}\right) \tag{2.10}$$

where

$$b(g,\Lambda/\rho_0) = \frac{2^{4g+1}}{\pi^2(4g+1)(\Lambda/\rho_0)^{4g}A(g,\Lambda/\rho_0)}. \tag{2.11}$$

This result constitutes an analytical confirmation of the empirical scaling form in Eq. (2.4) first proposed by Haque *et al.* [Zozulya et al., 2008, Haque et al., 2009], with $n=1$, where

$$a = -\ln\left[A(g,\Lambda/\rho_0)\right],\ \gamma = 4g+1. \tag{2.12}$$

2.4.1 Non-interacting spinless fermions

In the non-interacting limit when $K=1$ ($g=0$), Eq. (2.8) yields $A(0,\Lambda/\rho_0)=1$ and thus $a=0$ in agreement with previous calculations of the particle partition

EE for free fermions (FF) on a lattice [Zozulya et al., 2008] where it was found that $S_{2,FF}(n=1) = \ln N$. However, combining Eqs. (2.10)-(2.11) for $g = 0$ yields

$$S_2(n=1) \simeq \ln(N) + \frac{2}{\pi^2 N}. \tag{2.13}$$

in disagreement with the lattice result by a factor of $\mathcal{O}(N^{-1})$. To ensure that this discrepancy does not arise from the approximations made in expanding the integral in Eq. (2.7) we can return to the exact expression for the 1-RDM for non-interacting spinless fermions:

$$\rho_{1,FF}(x,x') = \frac{\sin(\pi\rho_0|x-x'|)}{\pi\rho_0 L|x-x'|}, \tag{2.14}$$

which leads to a soluble integral and analytic form for the EE in the spatial continuum:

$$S_{2,FF}(n=1) = \ln(N) - \ln\left\{\frac{2\left[N\pi\mathrm{Si}(N\pi) + \cos(\pi N) - 1\right]}{\pi^2 N}\right\} \tag{2.15}$$

where $\mathrm{Si}(z)$ is the sine integral. Expanding for large N recovers the asymptotic form in Eq. (2.13) which differs from the known lattice result.

2.4.2 Effects of boundary conditions

The origin of this $1/N$ difference between free spinless fermions in the continuum vs. the lattice is related to our neglect of finite-size boundary conditions when studying the asymptotic behavior of the second Rényi EE. To properly capture the finite-size effects of periodic boundary conditions we replace separations $|x-x'|$ with the chord length between two points on a ring of circumference L [Cazalilla, 2004]:

$$|x-x'| \to \frac{L}{\pi}\sin\left(\frac{\pi}{L}|x-x'|\right). \tag{2.16}$$

Using the finite-size corrected 1-RDM, the integral in Eq. (2.7) takes the form

$$f(N,g,\Lambda/\rho_0) = \frac{2}{N^2}\int_0^{N/2} dy \frac{\sin^2(\pi y)}{\sin^2(\frac{\pi y}{N})\left[1+\frac{N^2\Lambda^2}{\pi^2\rho_0^2}\sin^2(\frac{\pi y}{N})\right]^{2g}}. \tag{2.17}$$

where the effects of finite L will appear only in the prefactors of decaying terms in an asymptotic expansion. Employing Eq. (2.17) for free fermions with $g = 0$ we recover the known lattice result $S_{2,FF}(n=1) = \ln(N)$. For all subsequent comparisons with numerical data at finite g we employ the appropriately finite size corrected form of the 1-RDM when computing the Rényi entanglement entropy.

2.5 Exact diagonalization of the $t-V$ chain of spinless fermions

In order to test the validity of our main result in Eq. (2.10) for the $n = 1$ particle partition EE, we consider the $t-V$ model of N spinless fermions on a chain with M sites defined by the Hamiltonian

$$H = -t\sum_i \left(c_i^\dagger c_{i+1} + c_{i+1}^\dagger c_i\right) + V\sum_i n_i n_{i+1} \tag{2.18}$$

where $c_i^\dagger$ and c_i are the fermionic creation and annihilation operators at site i and $n_i = c_i^\dagger c_i$ is the occupation number. The model is parameterized by the nearest-neighbor hopping amplitude $t > 0$, and interaction strength V. We consider only the half-filled case ($M = 2N$) with periodic boundary conditions (PBC) for odd number of fermions N, while for even N we use antiperiodic boundary conditions (APBC) to avoid the otherwise degenerate ground state [Cazalilla, 2004] (See Fig. A.4). In order to make connection with the general TLL theory described above, we require a method to determine the parameter K from the microscopic $t - V$ model. This can be accomplished via the Jordan–Wigner transformation [Jordan and Wigner, 1928] which maps the $t - V$ model onto the XXZ spin-1/2 chain that is exactly solvable [Cloizeaux, 1966, Cloizeaux and Gaudin, 1966]. In the range $|V/t| < 2$, the system is known to be in the TLL phase, where the analytical form of K is given by

$$K = \frac{\pi}{2\cos^{-1}(-V/2t)}. \tag{2.19}$$

By increasing the repulsive interaction across $V/t = 2$ ($K = 1/2$), the system undergoes a continuous phase transition to a charge-density wave (CDW) phase. In contrast, the transition across $V/t = -2$ ($K \to \infty$) is a discrete one, where the fermions tend to form a single cluster.

Beginning with the non-interacting case ($V/t = 0$), the free fermionic Hamiltonian is diagonal in the momentum-space representation leading to a ground state that is a Slater determinant of the N lowest energy modes. The rank of the resulting n-RDM is $\binom{N}{n}$ and with equal eigenvalues [Zozulya et al., 2008], it follows (as introduced above) that all the Rényi EEs are equal to

$$S_{\alpha,FF}(n) = \ln \binom{N}{n}. \tag{2.20}$$

In the presence of interactions, we calculate the von Neumann ($\alpha = 1$) and the second ($\alpha = 2$) Rényi EEs from the ground state of Eq. (2.18) which we obtain via numerical exact diagonalization. The resulting n-RDM has maximum possible rank $\binom{M}{n}$ due to the indistinguishability of the $n < N$ particles in the partition, as opposed to $n!\binom{M}{n}$, the full dimension of the Hilbert space in the first quantized basis. Exploiting this symmetry, (for details, see **??**) we are able to study systems up to $M = 28$ sites, a considerable advancement over previous work [Haque et al., 2009]. The results are shown in Fig. 2.2 which demonstrates that the entanglement entropy $S_\alpha(n = 1)$ increases with increasing interaction strength $|V/t|$ up to a maximum of $S_{\alpha,FF}(n = 1) + \ln 2$ (for even N) in the limit $|V/t| \to \infty$ [Zozulya et al., 2008, Haque et al., 2009]. For attractive interactions, $S_\alpha(n = 1)$ displays a sharp increase around the first-order transition point $V/t = -2$. In contrast, $S_\alpha(n = 1)$ does not seem to be sensitive to the continuous transition at $V/t = 2$ [Zozulya et al., 2008]. However, when considering a macroscopic partition size $n = N/2$, we observe that $S_\alpha(n = N/2)$ develops a peak near $V/t = 2$ which appears to approach the critical point as we increase N (Fig. 2.2 (b)). Eventually, $S_\alpha(n = N/2)$ saturates to $\ln \binom{N}{N/2} + \ln 2$ in the limit $V/t \to \infty$, with details given in B.2.

We now turn to the TLL region $|V/t| < 2$, where we expect the scaling of the interaction contribution to the EE: $S_2(n = 1) - \ln(N)$, to be linear in $1/N^{4g+1}$ with

corrections of $\mathcal{O}(1/N^{4g+2})$ as in Eq. (2.10). To test this prediction, we rearrange Eq. (2.10) as:

$$\frac{S_2(n=1) - \ln(N) - a}{b} = N^{-(4g+1)} + \mathcal{O}\left(N^{-(4g+2)}\right). \tag{2.21}$$

and calculate $S_2(n=1)$ as a function of N using the ground state of $t-V$ model for different values of the interaction strength V/t, deep in the TLL phase (away from the phase transitions). For each interaction strength V/t, we compute $g = (K + K^{-1} - 2)/4$ using Eq. (2.19) and extract a and b from a linear fit to the $S_2(n=1) - \ln(N)$ vs $N^{-(4g+1)}$ data set. Next, we use the extracted coefficients to rescale $S_2(n=1) - \ln(N)$ according to Eq. (2.21). The results are illustrated in Fig. 2.3, where, for suitably large N, the data follows the straight line predicted by Eq. (2.21) with unit slope, verifying the TLL scaling form in Eq. (2.10). Deviations from linearity for smaller N arise due to finite size corrections of $\mathcal{O}(1/N^{4g+2})$.

Having understood the asymptotic scaling of the 1-particle partition Rényi EE with N, we now consider its dependence on the interaction strength g. This amounts to asking if the g-dependence of the scaling coefficients a and b for the $t-V$ model can be predicted from our continuum theory. To answer this question we calculate the second Rényi EE for $|V/t| < 2$ in the liquid phase at fixed N by evaluating the full integral in Eq. (2.17) numerically including all contributions from finite N. However, in order to compare the resulting particle EE with that obtained from the exact diagonalization, we need to identify the corresponding non-universal value of the ratio Λ/ρ_0 in the $t-V$ model. At half filling, the average particle density is $\rho_0 = 1/2x_0$ where x_0 is the lattice separation, while one estimates the ultraviolet cutoff Λ to be of the order of $1/x_0$, yielding $\Lambda/\rho_0 \approx 2$. The open and closed symbols in Fig. 2.4 show the exact diagonalization results for $S_2(n=1) - \ln(N)$ as a function of g for $N = 13$. The three lines correspond to the prediction from the TLL theory for slightly different values of the UV cutoff Λ. Due to the highly non-linear relationship between the interaction strength V/t and the TLL parameter K (Eq. 2.19), in combination with the sensitivity of the particle partition entanglement to the strength and nature of inter-particle interactions, it is no surprise that the EE in the $t-V$ model is a multi-valued function of the effective interaction parameter g for attractive and repulsive interactions. Clearly, high energy lattice-scale physics, not captured within the low energy TLL theory is responsible for this behavior. Moreover, recall that the ultraviolet cutoff, Λ, in Eq. (2.5), is proportional to the inverse of the effective range of the interaction [Dzyaloshinskii and Larkin, 1974]. Therefore, we expect Λ to exhibit a dependence on the nature and strength of the interaction, i.e., have K-dependence [Herdman and Del Maestro, 2015]. Considering such a dependence, we find that the $t-V$ model results for $S_2(n=1) - \ln(N)$ are bounded by the theoretically calculated ones using $\Lambda/\rho_0 = 1.7$ and 2.5 (Fig. 2.4). Note that both ratios are of order 2.

Testing the proposed leading order scaling of the particle partition EE in Eq. (2.4) with the partition size n in the TLL phase, requires the calculation of n-RDM with $n > 1$. While this can be done in principle using standard techniques [Giamarchi, 2004], the resulting evaluation of $S_2(n)$ requires performing $2n$ non-separable integrals. Even for the $n = 2$ we were not able to analytically extract the asymptotic scaling of Tr ρ_2^2. However, from numerical exact diagonalization of the $t-V$ model in the in the TLL phase we were able to calculate the Rényi EEs for partitions up to

$n = N/2 = 5$ for $N = 10$ as seen in Fig. 2.5. Our results are in agreement with previous calculations of $N = 6, n = 3$ [Zozulya et al., 2008] and strongly suggest that the leading term in the scaling of the Rényi EEs with n is indeed equal to the Rényi EE of free fermions, i.e., $\ln \binom{N}{n}$. Interactions introduce a correction term that increases with the partition size with a negative curvature (see Fig. 2.5 inset) such that both the leading order constant and finite-size power-law corrections to scaling both depend on n.

Finally we investigate the question of whether particle bipartition EE is sensitive to the ground state degeneracy known to occur in the $t - V$ model with periodic boundary conditions and an even number of sites. Introducing the inversion operator P [Kampf et al., 2003] defined by

$$Pc_i^\dagger P^\dagger = c_{M-i+1}^\dagger, \qquad i = 1, \cdots, M. \tag{2.22}$$

where P commutes with the Hamiltonian of the $t - V$ model in Eq. (2.18) for PBC, we can write the degenerate ground state as a superposition of the eigenstates of the inversion operator: $P|\Phi_\pm\rangle = \pm|\Phi_\pm\rangle$, i.e.,

$$|\Psi\rangle = \cos(\theta)|\Phi_+\rangle + \sin(\theta)|\Phi_-\rangle. \tag{2.23}$$

Here, we only consider a superposition with real coefficients that can be varied through the parameter $0 \leq \theta \leq \pi$ and study the dependence of the Rényi EEs on θ as seen in Fig. 2.6. Our numerical results for repulsive interactions with $N = 10$ show that $S_1(n = 1)$ oscillates with θ (Fig. 2.6 inset), where the maximum EE corresponds to $|\Psi\rangle$ being an eigenstate of P, i.e., $\theta = 0$ or $\theta = \pi/2$, and the minimum EE is obtained when both eigenstates $|\Phi_\pm\rangle$ contribute equally to $|\Psi\rangle$ (maximum uncertainty in P, $\theta = \pi/4, 3\pi/4$). Moreover, the difference between the lower and upper bound vanishes in the non-interacting limit and widens with increasing interaction strength up to $\ln 2$ in the limit $V/t \to \infty$ (see B.2). Interestingly, Fig. 2.6 shows that for $\theta = \pi/4$, $S_1(n = 1)$ exhibits a peak near the critical point ($V/t = 2$), while the $S_1(n = 1)$ dependence on V/t for $\theta = 0$ is very similar to that obtained from the non-degenerate ground state using APBC.

2.6 Conclusions

In this paper we have studied the finite size and interaction dependence of the particle partition Rényi entanglement entropies of a fermionic Tomonaga-Luttinger liquid and find that:

$$S_\alpha(n, N) = \ln \binom{N}{n} + a_\alpha(n) + \mathcal{O}\left(\frac{1}{N^{\gamma_\alpha(n)}}\right) \tag{2.24}$$

where n is the number of particles in the subsystem and α the Rényi index. This result is in agreement with the empirical prediction made in Ref. [Zozulya et al., 2007]. For the special case $n = 1$, $\alpha = 2$ we have determined the power of the finite size correction to the leading logarithm to be $\gamma_2(1) = K + K^{-1} - 1$ where K is the Luttinger parameter and confirmed this interaction dependence for the $t - V$ model by mapping it to the exactly solvable XXZ chain. The more general result for $n > 1$, $\alpha \neq 2$ in Eq. (2.24) is supported by extensive exact diagonalization

results on the lattice $t-V$ model of spinless fermions obtained on systems with up to $M = 28$ sites. This general scaling form can be contrasted with a bosonic Tomonaga-Luttinger liquid, where it was found [Herdman and Del Maestro, 2015] that $S_2(n,N) \simeq (n/K)\ln N + a_2'(n) + \mathcal{O}(1/N^{1-K^{-1}})$ which asymptotically recovers the free fermion result in the limit of hard-core bosons ($K \to 1^+$) using the fact that $\binom{N}{n} \approx N^n/n!$ for $N \gg n$.

The universality of the prefactor of the leading order logarithm in Eq. (2.24) demonstrates that due to the required anti-symmetrization of the N-particle wavefunction, fermions are always more entangled than bosons under a particle partition. This is consistent with what was numerically found for hard-core particles with variable anyonic statistics [Santachiara et al., 2007]. Such sensitivity to particle statistics and interaction dependence is absent in the asymptotic scaling of the spatial mode entanglement entropy for critical $(1+1)$-dimensional systems where the prefactor is universal and related to the central charge of the underlying conformal field theory [Calabrese and Cardy, 2004]. Thus, the particle partition entanglement appears to be a useful diagnostic of quantum correlations in many-body systems, and its logarithmic scaling with the total number of particles N highlights the potential utility of protocols [Killoran et al., 2014] that aim to transfer it to experimentally accessible mode entanglement.

An interesting open question remains on the origin and development with system size of the peak in the entanglement entropy in the ground state of the $t-V$ model near the continuous phase transition at $V/t = 2$ for macroscopic particle partitions with $n = N/2$ (Fig. 2.2 (b)). A careful finite-size analysis of this unexpected feature (due to the lack of any natural length scale describing the partition) would require moving beyond exact diagonalization and employing recently adapted hybrid Monte Carlo methods [Drut and Porter, 2015, Drut and Porter, 2016, Porter and Drut, 2016].

2.7 Acknowledgements

We thank P. Fendley and C. Herdman for enlightening discussions. The exact diagonalization code used in this work was adapted from one written by R. Melko and D. Iouchtchenko [cod,]. This research was supported in part by the National Science Foundation under Award No. DMR-1553991.

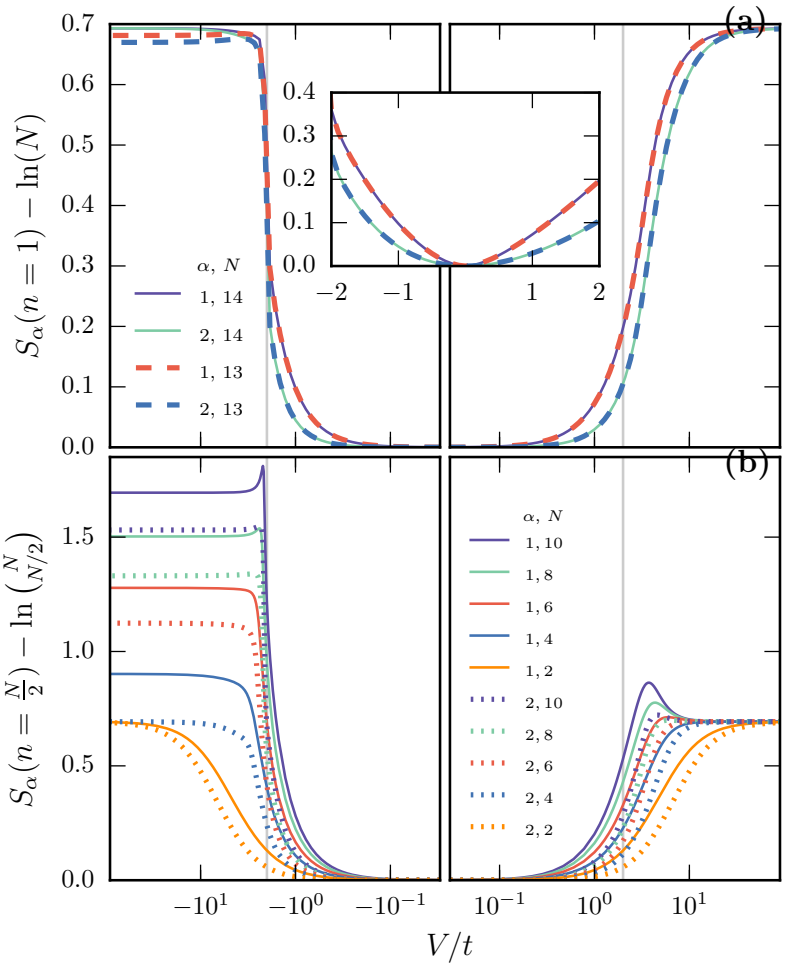

Figure 2.2: Interaction effects on the n-particle entanglement entropy $S_\alpha(n)$ for $\alpha = 1, 2$ in the ground state of the $t - V$ model. (a) $S_\alpha(n = 1) - \ln N$ vs V/t for $N = 13$ and 14 with periodic and anti-periodic boundary conditions, respectively. The light gray vertical lines mark the location of the known phase transitions at $V/t = \pm 2$. The subtracted $\ln(N)$ term is the one-particle entanglement entropy for free fermions. Inset: the Tomonaga-Luttinger liquid region where we expect the continuum theory to apply. (b) $S_\alpha(n = N/2) - \ln\binom{N}{N/2}$ vs V/t for *macroscpic* partitions with $1 \leq n \leq 5$ and anti-periodic boundary conditions. As $n \to N/2$, features appear near the phase transitions for $\alpha = 1$.

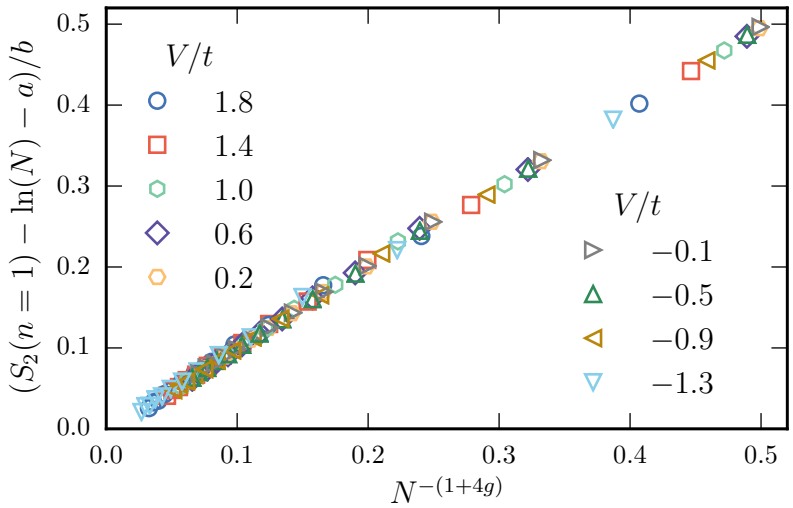

Figure 2.3: Finite size scaling of $S_2(n = 1) - \ln(N)$ with $N^{-(4g+1)}$ for $2 \leq N \leq 14$ confirming the empirical asymptotic scaling predicted by Zozulya *et al.* [Zozulya et al., 2007] and identifying the power of the leading finite size correction as $\gamma = 4g + 1$. The coefficients a and b depend on the interaction strength V/t and are calculated from a linear fit of the exact diagonalization data according to Eq. (2.10).

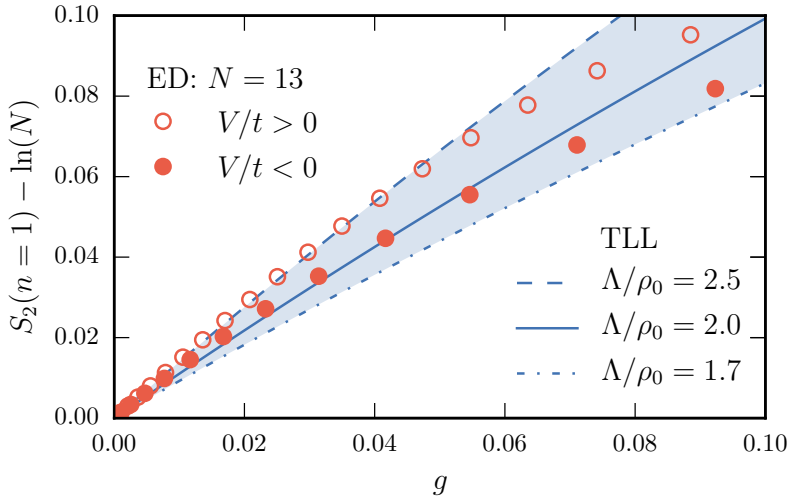

Figure 2.4: The effective interaction dependence of the 1-particle partition second Rényi entanglement entropy $S_2(n = 1) - \ln(N)$. Open (closed) points were computed via exact diagonalization of the $t - V$ model for $N = 13$ with repulsive (attractive) interactions. The lines show the prediction from the Tomonaga-Luttinger liquid theory for three different values of the ultraviolet cutoff Λ measured in units of the density ρ_0.

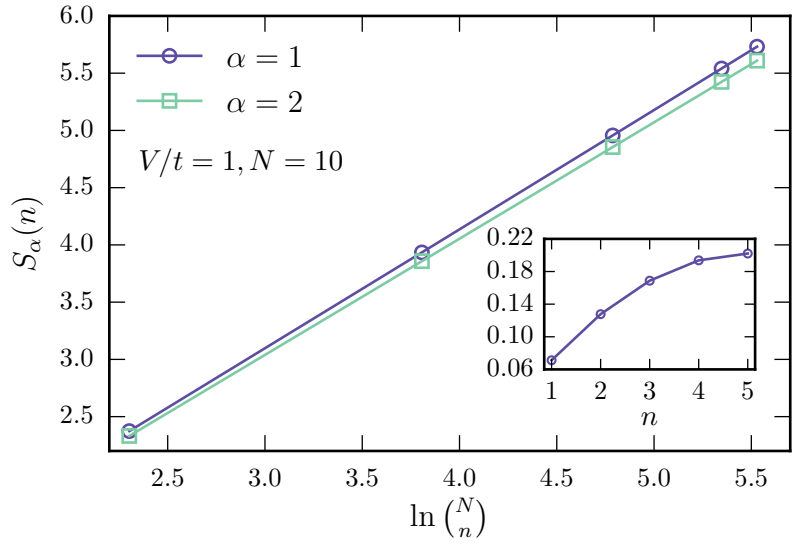

Figure 2.5: Scaling of $S_\alpha(n)$ with $\ln \binom{N}{n}$ for $\alpha = 1, 2$ in the ground state of the $t-V$ model with $V/t = 1$, $N = 10$, and for partition sizes $1 \leq n \leq 5$. Inset: Interaction contribution to the EE $(S_1(n) - \ln \binom{N}{n})$ vs n.

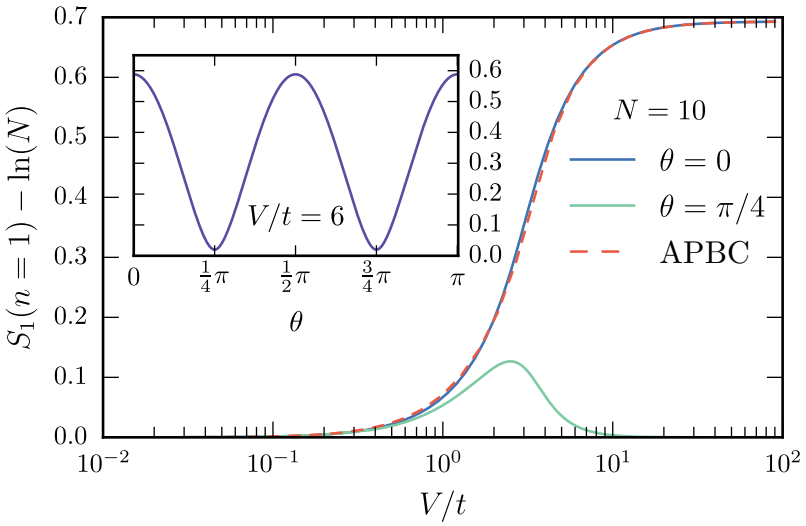

Figure 2.6: Effects of ground state degeneracy. The $S_2(n = 1) - \ln(N)$ dependence on V/t in the ground state of the $t-V$ model for $N = 10$. Solid lines represent results obtained from the degenerate ground state in Eq. (2.23) using PBC and $\theta = 0, \pi/4$ (see the text for details). The dashed line corresponds to the non-degenerate ground state for APBC. Inset: $S_2(n = 1) - \ln(N)$ vs θ for $V/t = 6$.

Chapter 3

Operational Entanglement Entropy in the tV Model

3.1 The operational entanglement

Consider some N-particle quantum state, in which the N particles are shared between spatial subregions A and B, or Alice and Bob, if you will. If Alice's and Bob's particles are entangled, this entanglement could be used as a resource for real world applications. Nevertheless, by using the traditional Von Neumann or Rényi Entanglement entanglement entropy, an overestimated measure of the physically available entanglement is obtained. This happens because for applications that rely on quantum entanglement, the particle number has to be conserved and these traditional measures do not account for this. To address this issue, Wiseman and Vaccaro [Wiseman and Vaccaro, 2003b] developed a measure known as Operational Entanglement (originally called Entanglement of Modes by the authors). The operational entanglement takes into account that the local particle number that are in Alice and Bob has to be conserved, giving a more physically accurate measure of entanglement.

3.1.1 Projecting onto subspaces of fixed local particle number

Knowing the density matrix of subregion A will suffice to calculate, for example, the spatial Rényi Entanglement Entropy. Nevertheless, to get the operational entanglement, simply knowing ρ_A is not enough. To recap, the spatial Rényi Entanglement Entropy is given by:

$$S_\alpha(\rho_A) = \frac{1}{1-\alpha} \log \operatorname{Tr} \rho_A^\alpha \tag{3.1}$$

Where α is the Rényi Index and ρ_A is the density matrix of subregion A. This calculation is still required to get operational entanglement but, as shall be seen, a few extra steps have to be taken to make sure that local particle number conservation is being satisfied. The first of these extra steps will be to project ρ_A to subspaces of local particle number. Projection operators can be written as diagonal matrices with ones on the columns corresponding to the subspace for which the projection is desired. Knowing this, the projection operators into subspaces of fixed local particle

numbers can be built rather simply. The projected reduced density matrix of A into the subspace of fixed local particle number n is obtained by:

$$\rho_{A,n} = \frac{1}{P_n}\hat{\Pi}_n \rho_A \hat{\Pi}_n \tag{3.2}$$

Where P_n is the probability of measuring an Alice state with n particles and $\hat{\Pi}_n$ is the projection operator onto the subspace of local particle number n.

After all this preamble, the operational entanglement can now be obtained. The operational entanglement is:

$$S_\alpha^{op}(\rho_A) = \sum_n P_n S(\rho_{A,n}) \tag{3.3}$$

Where the sum is carried over all possible local particle numbers that Alice may have. In other words, $n = 0, 1, ..., N - n_B$.

In the following section, analytical results of the operational entanglement entropy at differential interaction strength regimes in the tV model are derived.

3.2 Analytical results at various regimes of the tV model

In the tV model, the state of the system is exactly known in three different interaction strength regimes:

i) $V/t \to +\infty$

ii) $V/t \to +\infty$

iii) $V/t = -2$

Starting from the known states at these regimes, analytical values for the operational entanglement were calculated. The results will be discussed in this section.

3.2.1 Infinitely repulsive interaction

The state in this limit is known as a charged density wave (CDW). In the occupation number basis, the CDW state is:

$$|\Psi\rangle_{CDW} = \frac{1}{\sqrt{2}}[|101010...\rangle + |010101...\rangle]$$

Where 1 denotes that the site is occupied and 0, that it is vacant. The coefficient before the bracket is a normalization constant. As will be shown, the operational entanglement for this state is dependent on the parity of the total number of particles N. Up next, the result for even N will be derived.

3.2.1.1 Even N

In the following calculations, again, the system will be partitioned into spatial subregions A and B, both containing the same number of sites. In other words, if the total number of sites in the $t - V$ chain is L, then the partition size will be $l = \frac{L}{2}$.

In the case of even particle number N, the CDW state will have the same number of particles in each subregion A and B:

$$|\Psi\rangle_{N_{Even}} = \frac{1}{\sqrt{2}}[|\underbrace{1010...}_{\frac{N}{2}particles}, \underbrace{1010...}_{\frac{N}{2}particles}\rangle + |\underbrace{0101...}_{\frac{N}{2}particles}, \underbrace{0101...}_{\frac{N}{2}particles}\rangle] \tag{3.4}$$

As a reminder, labels left to the comma correspond to spatial subregion A, while those to the right correspond to B.

The full density matrix ρ_{AB} takes the form:

$$\begin{aligned}\rho_{AB} &= |\Psi\rangle_{N_{Even}}\langle\Psi|_{N_{Even}} \\ &= \frac{1}{2}|0101..., 0101\rangle\langle 0101..., 0101...| + \frac{1}{2}|0101..., 0101\rangle\langle 1010..., 1010...| \\ &+ \frac{1}{2}|1010..., 1010\rangle\langle 0101..., 0101...| + \frac{1}{2}|1010..., 1010\rangle\langle 1010..., 1010...|\end{aligned} \tag{3.5}$$

Recall that to calculate the entanglement entropies, it is necessary to obtain the reduced density matrix of subsystem A. Taking the partial trace with respect to B, the reduced density matrix of A is obtained:

$$\rho_A = \mathrm{Tr}_B\, \rho_{AB} \quad = \sum_n {}_B\langle n|\Psi\rangle\langle\Psi|n\rangle_B \tag{3.6}$$

Where the summation is carried over all possible states that B can be found in. In this case, there are only two possible B states: $n = |0101...\rangle_B$ and $|1010...\rangle_B$Thus, taking the partial trace respect to B of Eq. (2.5):

$$\rho_A = \frac{1}{2}|0101...\rangle_A\langle 0101...|_A + \frac{1}{2}|1010...\rangle_A\langle 1010...|_A \tag{3.7}$$

Notice that some of the terms have vanished due to the orthonormality of the states. At this point, it will be convenient for purposes of illustration to rewrite the reduced density matrix of A in actual matrix form rather than in Dirac or Bra-Ket notation:

$$\rho_A = \begin{pmatrix} \frac{1}{2} & 0 \\ 0 & \frac{1}{2} \end{pmatrix} \tag{3.8}$$

For spatial entanglement, ρ_A would suffice, but for operational entanglement, the matrix has to be projected onto the various subspaces of fixed local particle number in A. In this case, both of the states share the same local particle number. That is, the states: $|1010...\rangle_A$ and $|0101...\rangle_A$ both have local particle number $n = \frac{N}{2}$. Thus only one projection operator is needed. In fact, the operator needed here turns out to be equal to the identity operator:

$$\hat{\Pi}_{n=\frac{N}{2}} = \begin{pmatrix} 1 & 0 \\ 0 & 1 \end{pmatrix} = \hat{I} \tag{3.9}$$

The probability of measuring a state with local particle number $n = \frac{N}{2}$ is equal to one. Thus, the projected density matrix of A onto the subspace of $n = \frac{N}{2}$ is:

$$\rho_{A,\frac{N}{2}} = \frac{1}{P_{\frac{N}{2}}}\hat{\Pi}_{\frac{N}{2}}\rho_A\hat{\Pi}_{\frac{N}{2}} \tag{3.10}$$

$$= \hat{I}\rho_A\hat{I} \tag{3.11}$$

$$\rho_{A,\frac{N}{2}} = \rho_A = \begin{pmatrix} \frac{1}{2} & 0 \\ 0 & \frac{1}{2} \end{pmatrix} \tag{3.12}$$

The reduced, projected and normalized reduced density matrix of A is now known and can be substituted into Eq. 2.3 to calculate the operational entanglement entropy:

$$S_\alpha^{op}(\rho_A) = \sum_n P_n S_\alpha(\rho_{A,n}) \tag{3.13}$$

$$= \frac{1}{1-\alpha}\log \mathrm{Tr}\,\rho_{A,\frac{N}{2}}^\alpha \tag{3.14}$$

$$= \frac{1}{1-\alpha}\log \mathrm{Tr}\begin{pmatrix} (\frac{1}{2})^\alpha & 0 \\ 0 & (\frac{1}{2})^\alpha \end{pmatrix} \tag{3.15}$$

$$= \frac{1}{1-\alpha}\log(\frac{1}{2^\alpha}+\frac{1}{2^\alpha}) \tag{3.16}$$

$$= \frac{1}{1-\alpha}\log 2^{(1-\alpha)} \tag{3.17}$$

$$S_\alpha^{op}(\rho_A) = \log 2 \tag{3.18}$$

Thus, for even N and $V/t \to +\infty$, the operational entanglement converges to $\log 2$. Up next, the result for odd N will be derived.

3.2.1.2 Odd N

The most general quantum state becomes:

$$|\Psi\rangle_{N_{Odd}} = \frac{1}{\sqrt{2}}[|\underbrace{...101}_{\frac{N+1}{2}particles}, \underbrace{010...}_{\frac{N-1}{2}particles}\rangle + |\underbrace{...010}_{\frac{N-1}{2}particles}, \underbrace{101...}_{\frac{N+1}{2}particles}\rangle] \tag{3.19}$$

Note that now when doing an equal spatial bipartition, one of the subregions will have one more particle than the other, unlike the even particle case in which both subregions had the same number of particles. Specifically, one of the subregions will have $\frac{N+1}{2}$ and the other, $\frac{N-1}{2}$. This implies that ρ_A will have to be projected onto the space of local particle number $\frac{N+1}{2}$ and $\frac{N-1}{2}$. But before doing that, again the full body density matrix is needed:

$$\begin{aligned}\rho_{AB} &= |\Psi\rangle_{N_{Even}}\langle\Psi|_{N_{Even}} \\ &= \frac{1}{2}|...101,010...\rangle\langle...101,010...| + \frac{1}{2}|...101,010...\rangle\langle...010,101...| \\ &+ \frac{1}{2}|...010,101...\rangle\langle...101,010...| + \frac{1}{2}|...010,101...\rangle\langle...010,101...|\end{aligned} \tag{3.20}$$

The possible B states are: $n = |101...\rangle, |010...\rangle$ with $\frac{N+1}{2}$ and $\frac{N-1}{2}$ particles, respectively. Taking the partial trace respect to B, the reduced density matrix of A becomes:

$$\rho_A = \frac{1}{2}|101...\rangle_A\langle 101...|_A + \frac{1}{2}|010...\rangle_A\langle 010...|_A \tag{3.21}$$

Once again, it may be more illustrative to rewrite in matrix form. Defining an orthonormal basis $|101...\rangle_A = \begin{pmatrix}1\\0\end{pmatrix}$ and $|010...\rangle_A = \begin{pmatrix}0\\1\end{pmatrix}$ the reduced density matrix of A becomes:

$$\rho_A = \begin{pmatrix}\frac{1}{2} & 0\\ 0 & \frac{1}{2}\end{pmatrix} \tag{3.22}$$

The simple projection operators onto $\frac{N+1}{2}$ and $\frac{N-1}{2}$ particle space in this basis are:

$$\hat{\Pi}_{\frac{N+1}{2}} = \begin{pmatrix}1 & 0\\ 0 & 0\end{pmatrix}, \hat{\Pi}_{\frac{N-1}{2}} = \begin{pmatrix}0 & 0\\ 0 & 1\end{pmatrix} \tag{3.23}$$

Applying these projections to ρ_A and choosing the probability such that the trace of each matrix is unity (normalization):

$$\rho_{A,\frac{N+1}{2}} = \begin{pmatrix}1 & 0\\ 0 & 0\end{pmatrix} \text{ with probability } P_{\frac{N+1}{2}} = \frac{1}{2} \tag{3.24}$$

and

$$\rho_{A,\frac{N-1}{2}} = \begin{pmatrix}0 & 0\\ 0 & 1\end{pmatrix} \text{ with probability } P_{\frac{N-1}{2}} = \frac{1}{2} \tag{3.25}$$

Substituting into the operational entanglement equation (Eq. 2.3):

$$S_\alpha^{op}(\rho_A) = \sum_n P_n S_\alpha(\rho_{A,n}) \tag{3.26}$$

$$= (\frac{1}{2})\frac{1}{1-\alpha}\log \mathrm{Tr}\,\rho_{A,\frac{N+1}{2}}^\alpha + (\frac{1}{2})\frac{1}{1-\alpha}\log \mathrm{Tr}\,\rho_{A,\frac{N-1}{2}}^\alpha \tag{3.27}$$

$$= \frac{1}{2-2\alpha}[\log \mathrm{Tr}\begin{pmatrix}1^\alpha & 0\\ 0 & 0\end{pmatrix} + \log \mathrm{Tr}\begin{pmatrix}0 & 0\\ 0 & 1^\alpha\end{pmatrix}] \tag{3.28}$$

$$= \frac{1}{2-2\alpha}[\underbrace{\log 1 + \log 1}_{=0}] \tag{3.29}$$

$$S_\alpha^{op}(\rho_A) = 0 \tag{3.30}$$

Therefore, the operational entanglement vanishes in the infinite repulsion limit ($V/t \to +\infty$) and odd number of particles in the system.

Summarizing:

$$\lim_{V\to+\infty} S_\alpha^{op} = \begin{cases}\log 2 & \text{if } N \text{ is even}\\ 0 & \text{if } N \text{ is odd}\end{cases} \tag{3.31}$$

3.2.2 Infinitely attractive interaction

In this section, an analytical result will be derived at half-filling ($L = 2N$) and partition size equal to the half the number of sites ($\ell = \frac{L}{2}$) for $V/t \to -\infty$. After arriving to the half-filling result, a general result, for any filling fraction and partition size, will be also derived.

3.2.2.1 Half-filling

In the infinitely attractive regime of the tV model, $V/t \to -\infty$, the fermions cluster together. The most general state in this regime is:

$$|\Psi\rangle_{PSS} = \frac{1}{\sqrt{L}}[|\underbrace{111...111}_{Nparticles},\underbrace{000...000}_{Nvacancies}\rangle + |011...111, 100...000\rangle + |001...111, 110...000\rangle + ... + |\underbrace{000...000}_{Nvacancies},\underbrace{111...111}_{Nparticles}\rangle + |100...000, 011...111\rangle + ...|111...110, 000...001\rangle] \tag{3.32}$$

This state is known as a phase separated solid (PSS). There are a total of L possible configurations, hence the normalization constant $\frac{1}{\sqrt{L}}$.

In an effort to simplify the notation while keeping the calculation general, the A or B states will be relabeled as:

$$\begin{aligned}
|111...111\rangle &\to |N\rangle \\
|011...111\rangle &\to |N-1\rangle \\
|001...111\rangle &\to |N-2\rangle \\
&\vdots \\
|000...011\rangle &\to |2\rangle \\
|000...001\rangle &\to |1\rangle \\
|000...000\rangle &\to |0\rangle
\end{aligned}$$

There is still one flaw with this notation. A $|N-1\rangle$ state could represent either $|011...111\rangle$ or $|111...110\rangle$. In other words, even though they have the same local particle number $N-1$, the configurations themselves are different. One way in which this problem can be circumvented is by adding a subscript to the label to represent distinct configurations. Since particle number will only be shared between two distinct particle configurations, using subscripts of 1 and 2 seems natural. For example: $|011...111\rangle \to |(N-1)_1\rangle$ and $|111...110\rangle \to |(N-1)_2\rangle$. $|\Psi\rangle_{PSS}$ now becomes:

$$|\Psi\rangle_{PSS} = \frac{1}{\sqrt{L}}[|N,0\rangle + |(N-1)_1, 1_1\rangle + |(N-2)_1, 2_1\rangle + ... + |0, N\rangle + |1_2, (N-1)_2\rangle + ...|(N-1)_2, 1_2\rangle] \tag{3.33}$$

Taking the outer product of Eq. 2.33 with itself, the full body density matrix is obtained:

$$\rho_{AB} = |\Psi\rangle_{PSS}\langle\Psi|_{PSS} = \begin{pmatrix} \frac{1}{L} & \frac{1}{L} & \dots & \frac{1}{L} \\ \frac{1}{L} & \frac{1}{L} & \dots & \frac{1}{L} \\ \vdots & \vdots & \vdots & \vdots \\ \frac{1}{L} & \frac{1}{L} & \dots & \frac{1}{L} \end{pmatrix} \tag{3.34}$$

The full body density matrix is of size LxL with all entries equal to $\frac{1}{L}$. Before proceeding, the basis of this matrix should be described. Columns (from left to right) and rows (from top to bottom) are arranged as:
$|N,0\rangle, |0,N\rangle, |(N-1)_1,1_1\rangle, |(N-1)_2,1_2\rangle, |(N-2)_1,2_1\rangle, |(N-2)_2,2_2\rangle, ...,$
$|2_1,(N-2)_1\rangle, \rangle, |2_2,(N-2)_2\rangle, \rangle, |1_1,(N-1)_1\rangle, \rangle, |1_2,(N-1)_2\rangle$. Notice that configurations that share local particle number have been paired up next to each other. The first two states are exceptions, as their subregions never share the same local particle number with subregions of any other state. Now that the basis has been explained, it's time to get the reduced density matrix of A.

Taking the partial trace with respect to B of Eq. 2.34:

$$\rho_A = \begin{pmatrix} \frac{1}{L} & 0 & \dots & 0 & 0 \\ 0 & \frac{1}{L} & \dots & 0 & 0 \\ \vdots & \vdots & \ddots & \vdots & \vdots \\ 0 & 0 & \dots & \frac{1}{L} & 0 \\ 0 & 0 & \dots & 0 & \frac{1}{L} \end{pmatrix} \tag{3.35}$$

And in the hopes of being as explicit as possible, the rows and columns correspond to the following configurations and in the following order: $|N\rangle, |0\rangle, |(N-1)_1\rangle, |(N-1)_2\rangle, |(N-2)_1\rangle, |(N-2)_2\rangle, ..., |2_1\rangle, |2_2\rangle, |1_1\rangle, |1_2\rangle$

Now, ρ_A has to be projected onto the subspaces of local particle numbers. The allowed local particle numbers are: $n = N, N-1, N-2....2, 1, 0$. So a total of $\frac{M}{2}+1$ projections need to be done. There is a projection onto the subspace of $n = 0$, one onto $n = N$ and $\frac{M}{2}-1$ onto the remaining subspaces. The $\frac{M}{2}$ was obtained due to the pairs of states that share local particle number: $|(N-1)_1\rangle$ with $|(N-1)_2\rangle, |(N-2)_1\rangle$ with $|(N-2)_2\rangle$ and so on and so forth. The 1 is subtracted because the pair of states $|0\rangle$ and $|N\rangle$ don't share local particle number.

The projection operators for $n = 0$ and $n = N$ become:

$$\hat{\Pi}_N = \begin{pmatrix} 1 & 0 & \dots & 0 & 0 \\ 0 & 0 & \dots & 0 & 0 \\ \vdots & \vdots & \ddots & \vdots & \vdots \\ 0 & 0 & \dots & 0 & 0 \\ 0 & 0 & \dots & 0 & 0 \end{pmatrix}, \hat{\Pi}_0 = \begin{pmatrix} 0 & 0 & \dots & 0 & 0 \\ 0 & 1 & \dots & 0 & 0 \\ \vdots & \vdots & \ddots & \vdots & \vdots \\ 0 & 0 & \dots & 0 & 0 \\ 0 & 0 & \dots & 0 & 0 \end{pmatrix} \tag{3.36}$$

For the remaining $\frac{M}{2}-1$ states, there will be two consecutive non-zero entries in the diagonal. For example:

$$\hat{\Pi}_{N-1} = \begin{pmatrix} 0 & & & & & & & \\ & 0 & & & & & & \\ & & 1 & & & & & \\ & & & 1 & & & & \\ & & & & 0 & & & \\ & & & & & 0 & & \\ & & & & & & \ddots & \\ & & & & & & & 0 \end{pmatrix} \tag{3.37}$$

$$\hat{\Pi}_{N-2} = \begin{pmatrix} 0 & & & & & & & \\ & 0 & & & & & & \\ & & 0 & & & & & \\ & & & 0 & & & & \\ & & & & 1 & & & \\ & & & & & 1 & & \\ & & & & & & \ddots & \\ & & & & & & & 0 \end{pmatrix}, \hat{\Pi}_1 = \begin{pmatrix} 0 & & & & & & & \\ & 0 & & & & & & \\ & & 0 & & & & & \\ & & & 0 & & & & \\ & & & & 0 & & & \\ & & & & & 0 & & \\ & & & & & & \ddots & \\ & & & & & & & 1 \end{pmatrix} \tag{3.38}$$

Notice from the form of the projection operators that the projected reduced density matrices will be similar to each other but with the two non-zero entries shifted correspondingly in the diagonal. Thus taking the projection onto $n = N - 1$ of ρ_A:

$$\begin{aligned} \rho_{A,N-1} &= \frac{1}{P_{N-1}} \hat{\Pi}_{N-1} \rho_A \hat{\Pi}_{N-1} \\ \rho_{A,N-1} &= \frac{1}{P_{N-1}} \begin{pmatrix} 0 & & & & & & & \\ & 0 & & & & & & \\ & & \frac{1}{L} & & & & & \\ & & & \frac{1}{L} & & & & \\ & & & & 0 & & & \\ & & & & & 0 & & \\ & & & & & & \ddots & \\ & & & & & & & 0 \end{pmatrix} \end{aligned} \tag{3.39}$$

The probability of measuring a state with local particle number $N - 1$ can be obtained from normalization:

$$\operatorname{Tr} \rho_{A,N-1} = 1 \implies \frac{1}{P_{N-1}} \frac{2}{L} = 1 \implies P_{N-1} = \frac{2}{L} \tag{3.40}$$

Thus the projection onto $n = N - 1$ of ρ_A is:

$$\rho_{A,N-1} = \begin{pmatrix} 0 & & & & & & & \\ & 0 & & & & & & \\ & & \frac{1}{2} & & & & & \\ & & & \frac{1}{2} & & & & \\ & & & & 0 & & & \\ & & & & & 0 & & \\ & & & & & & \ddots & \\ & & & & & & & 0 \\ & & & & & & & & 0 \end{pmatrix} ; \text{ with probability } P_{N-1} = \frac{2}{L} \quad (3.41)$$

For $n = N - 2$:

$$\rho_{A,N-2} = \begin{pmatrix} 0 & & & & & & & \\ & 0 & & & & & & \\ & & 0 & & & & & \\ & & & 0 & & & & \\ & & & & \frac{1}{2} & & & \\ & & & & & \frac{1}{2} & & \\ & & & & & & \ddots & \\ & & & & & & & 0 \\ & & & & & & & & 0 \end{pmatrix} ; \text{ with probability } P_{N-2} = \frac{2}{L} \quad (3.42)$$

and so on and so forth.

Similarly, $\rho_{A,N}$ and $\rho_{A,0}$ become:

$$\rho_{A,N} = \begin{pmatrix} 1 & & & & & & & \\ & 0 & & & & & & \\ & & 0 & & & & & \\ & & & 0 & & & & \\ & & & & 0 & & & \\ & & & & & 0 & & \\ & & & & & & \ddots & \\ & & & & & & & 0 \\ & & & & & & & & 0 \end{pmatrix}, \rho_{A,0} = \begin{pmatrix} 0 & & & & & & & \\ & 1 & & & & & & \\ & & 0 & & & & & \\ & & & 0 & & & & \\ & & & & 0 & & & \\ & & & & & 0 & & \\ & & & & & & \ddots & \\ & & & & & & & 0 \\ & & & & & & & & 0 \end{pmatrix} \quad (3.43)$$

with probabilities $P_N = P_0 = \frac{1}{L}$
Finally, the operational entanglement is:

$$S_\alpha^{op}(\rho_A) = \sum_n P_n S_\alpha(\rho_{A,n}) \tag{3.44}$$

$$= \frac{1}{1-\alpha}[\frac{1}{L}\log \mathrm{Tr}\,\rho_{A,N}^\alpha + \frac{1}{L}\log \mathrm{Tr}\,\rho_{A,0}^\alpha + \frac{2}{L}\log \mathrm{Tr}\,\rho_{A,N-1}^\alpha \tag{3.45}$$

$$+ \frac{2}{L}\log \mathrm{Tr}\,\rho_{A,N-2}^\alpha + \cdots + \frac{2}{L}\log \mathrm{Tr}\,\rho_{A,2}^\alpha + \frac{2}{L}\log \mathrm{Tr}\,\rho_{A,1}^\alpha] \tag{3.46}$$

$$= \frac{1}{L-L\alpha}[\underbrace{\log 1}_{=0} + \underbrace{\log 1}_{=0} + 2\log(\frac{1}{2^\alpha} + \frac{1}{2^\alpha}) \tag{3.47}$$

$$+ 2\log(\frac{1}{2^\alpha} + \frac{1}{2^\alpha}) + \cdots + 2\log(\frac{1}{2^\alpha} + \frac{1}{2^\alpha}) + 2\log(\frac{1}{2^\alpha} + \frac{1}{2^\alpha})] \tag{3.48}$$

$$= \frac{2}{L-L\alpha}\underbrace{[\log 2^{(1-\alpha)} + \log 2^{(1-\alpha)} + \cdots + \log 2^{(1-\alpha)} + \log 2^{(1-\alpha)}]}_{\frac{L}{2}-1 \text{ terms}} \tag{3.49}$$

$$= (\frac{L}{2} - 1)(\frac{2}{L})\log 2^{\frac{1-\alpha}{1-\alpha}} \tag{3.50}$$

$$= (\frac{L-2}{2})(\frac{2}{L})\log 2;\ \text{recall that } L = 2N \tag{3.51}$$

$$S_\alpha^{op}(\rho_A) = \frac{N-1}{N}\log 2 \tag{3.52}$$

3.2.2.2 Analytical result for any filling fraction and partition size

The analytical result obtained above for the operational entanglement entropy in the infinitely attractive regime corresponds to the special case of half-filling ($N = \frac{L}{2}$) and equal spatial bipartitions ($\ell_A = \ell_B = \frac{L}{2}$). Nevertheless, a generalized result can be obtained for ant filling fraction and partition size by counting the number of projected reduced density matrices ($\rho_{A,n}$) that will contribute to the operational entanglement. As it will be shown, the number of contributing matrices will depend on how the quantities ℓ_A, ℓ_B, N & $N^c = L - N$ relate to each other. Demonstration of the following cases will suffice to get the general result:

$$i)\ell_A < N < \ell_B \tag{3.53}$$

$$ii)\ell_B < N < \ell_A \tag{3.54}$$

$$iii)N < \ell_A < \ell_B \tag{3.55}$$

$$iv)\ell_A < \ell_B < N \tag{3.56}$$

These four cases actually imply other cases and, in the end, all possible relations between the four parameters should be covered.

Case $i)$ $\ell_A < N < \ell_B$:

The condition here is that the size of the subregion A should be less than the total number of particles N and the size of the subregion B should be greater than both of these quantities. Under such conditions, particle configurations in which B is empty are not possible, since A is too small too fit them all. Two other configurations that will not contribute to the operational entanglement are when A is full ($n_A = \ell_A$) and when it is empty ($n_A = 0$). There is only one possible way of distributing the

particles in partition A if it is full and likewise if it is empty. As it was seen in the previous section, then the corresponding projected reduced density matrices ρ_{A,ℓ_A} and $\rho_{A,0}$ have only one nonzero eigenvalue which, after normalization, becomes 1. Thus, $\ln \rho^{\alpha}_{A,\ell_A} = \ln \rho^{\alpha}_{A,0} = 0$. There are a total of $\ell_A + 1$ possible local particle numbers (n_A) and since $n_A = \ell_A$ and $n_A = 0$ do not contribute, there are actually $\ell_A - 1$ contributing projected reduced density matrices. All such projected density matrix will have the form:

$$\rho_{A,n} = \begin{pmatrix} \frac{1}{L} & 0 \\ 0 & \frac{1}{L} \end{pmatrix} \tag{3.57}$$

The two diagonal elements come from the two configurations that have the same local particle number n. Technically, these projected reduced density matrices originally have the same dimensions as those in Eqs.$2.37-2.39, 2.41-2.43$. Nevertheless, rows and columns that only have zero entries have been thrown out for compactness. Normalizing:

$$\rho_{A,n} = \frac{1}{P_n} \begin{pmatrix} \frac{1}{2} & 0 \\ 0 & \frac{1}{2} \end{pmatrix}; P_n = \frac{2}{L} \tag{3.58}$$

Thus, the operational entanglement becomes:

$$S^{op}_{\alpha}(\ell_A, L) = (\ell_A - 1)\frac{2}{L}\ln 2 \tag{3.59}$$

Case *ii*) $\ell_B < N < \ell_A$:

This time, partition B is the one that can never be empty. Barring that, the argument is exactly the same as *i*) and thus:

$$S^{op}_{\alpha}(\ell_B, L) = (\ell_B - 1)\frac{2}{L}\ln 2 \tag{3.60}$$

Case *iii*) $N < \ell_A < \ell_B$:

In contrast to *i*) and *ii*), now the particles may all be in A or all in B. Nevertheless, in such instances, there is only a single possible configuration of the other partition, that in which it's empty. Thus, the projected reduced density matrices $\rho_{A,N}$ and $\rho_{A,0}$ have only one nonzero eigenvalue and, thus, do not contribute to the operational entanglement. Barring these two, there are then $N - 1$ projected reduced density matrices that do contribute. They all have the same form as the ones of *i*) and *ii*), that is, $2x2$ diagonal matrices (after throwing out all unnecessary zeroes) with 2 eigenvalues $\frac{1}{2}$ (after normalizing) and probabilities $P_n = \frac{2}{L}$. Thus:

$$S^{op}_{\alpha}(N, L) = (N - 1)\frac{2}{L}\ln 2 \tag{3.61}$$

Case *iv*) $\ell_A < \ell_B < N$:

Here, no partition will ever be empty. The maximum allowed particle number in A is going to be $n_A = \ell_A$ and the smallest one, $n_A = N - \ell_B$. The partition size of B is subtracted from N because the minimum n_A corresponds to a fully occupied partition B, that is $n_B = \ell_B$. The 'leftover' particles on A will hence be the total particle number minus those fully occupying B. Notice in all the previous examples that the total number of projected reduced density matrix is equal to the difference between max and min allowed particle number n_A plus 1. That is:

$$\text{Total Projected Reduced Density Matrices} = (n_A)_{max} - (n_A)_{min} + 1 \tag{3.62}$$

And for this case,

$$\begin{aligned}
\text{Total Projected Reduced Density Matrices} &= (n_A)_{max} - (n_A)_{min} + 1 && (3.63)\\
&= \ell_A - (N - \ell_B) + 1 && (3.64)\\
&= \underbrace{\ell_A + \ell_B}_{L} - N + 1 && (3.65)\\
\text{Total Projected Reduced Density Matrices} &= L - N + 1 && (3.66)
\end{aligned}$$

Let $L - N \equiv N^c$. The total number of contributing projected reduced density matrices is:

$$\begin{aligned}
\text{Contributing Matrices} &= \text{Total Matrices} - 2 && (3.67)\\
&= (N^c + 1) - 2 && (3.68)\\
\text{Contributing Matrices} &= N^c - 1 && (3.69)\\
& && (3.70)
\end{aligned}$$

the operational entanglement then becomes:

$$S_\alpha^{op}(N^c, L) = (N^c - 1)\frac{2}{L}\ln 2 \tag{3.71}$$

The operational entanglement at the infinitely attractive regime has now been obtained for conditions $i) - iv)$. Notice that it always has the form:

$$S_\alpha^{op}(x, L) = (x - 1)\frac{2}{L}\ln 2 \tag{3.72}$$

where x could be ℓ_A, ℓ_B, N or N^c. But how to determine which of these variables to choose? Recalling that $L - N = N^c, L - \ell_A = \ell_B$ and $L - \ell_B = \ell_A$, extra inequalities can be obtained from $i) - iv)$ that relate the four variables:

$$\begin{aligned}
&i)\ell_A < N < \ell_B \implies \ell_B > N^c > \ell_A \implies \ell_A \text{ is the smallest} && (3.73)\\
&ii)\ell_B < N < \ell_A \implies \ell_A > N^c > \ell_B \implies \ell_B \text{ is the smallest} && (3.74)\\
&iii)N < \ell_A < \ell_B \implies N^c > \ell_B > \ell_A \implies N \text{ is the smallest} && (3.75)\\
&iv)\ell_A < \ell_B < N \implies \ell_B > \ell_A > N^c \implies N^c \text{ is the smallest} && (3.76)\\
& && (3.77)
\end{aligned}$$

From the above set of inequalities, note that the smallest between the four variables in each case, also happens to be the variable that is substituted for x. Thus, in a more compact form, the generalized operational entanglement at the infinitely attractive regime is:

$$S_\alpha^{op}(x, L) = \frac{2(x-1)}{L}\ln 2;\ \text{where } x = \min \ell_A, \ell_B, N, N^c \tag{3.78}$$

3.2.3 First order phase transition

At $\frac{V}{t} = -2$, the tV-Model undergoes a first order phase transition from Luttinger Liquid to Phase Separated Solid. The operational entanglement at this interaction strength vanishes and then suddenly increases and converges to the previously derived limit ($\frac{N-1}{N} \ln 2$) as the attraction gets stronger. In this section, it will be shown that the operational entanglement vanishes at the first order phase transition.

At $\frac{V}{t} = -2$, and half-filling ($N = \frac{L}{2}$), the state of the system is a equiprobable superposition of all possible configurations. There are a total of $\binom{L}{N}$ possible configurations. Thus, the general state can be written as:

$$|\Psi\rangle = \frac{1}{\sqrt{\binom{L}{N}}} \sum_{i=1}^{\binom{L}{N}} |\phi_i\rangle \tag{3.79}$$

where $|\phi_i\rangle$ denotes a distinct particle configuration and the pre-factor is a normalization constant. Now that the state at $\frac{V}{t} = -2$ is known, the full and, hence, reduced density matrices can be obtained. Up next, their resulting general structure will be discussed.

For simplicity, let $\frac{1}{\sqrt{\binom{L}{N}}} \equiv C$. For particle sub-sectors of $n_A = 0$ and $n_A = N$, the projected reduced density matrices become:

$$\rho_{A,N} = \frac{1}{P_N} \begin{pmatrix} C & \dots & 0 \\ \vdots & 0 & \vdots \\ 0 & \dots & 0 \end{pmatrix} \tag{3.80}$$

with probability $P_N = C$. And,

$$\rho_{A,0} = \frac{1}{P_0} \begin{pmatrix} 0 & \dots & 0 \\ \vdots & 0 & \vdots \\ 0 & \dots & C \end{pmatrix} \tag{3.81}$$

also with probability $P_0 = C$.

For particle number sub-sectors of $1 \leq n \leq N-1$, the projected reduced density matrices become square matrices of size NxN with all entries being NC^2:

$$\rho_{A,n} = \frac{1}{P_n} \begin{pmatrix} NC^2 & \dots & NC^2 \\ \vdots & NC^2 & \vdots \\ NC^2 & \dots & NC^2 \end{pmatrix} \tag{3.82}$$

with probabilities $P_n = N(NC^2) = N^2C^2$.

In summary, the normalized projected reduced density matrices are:

$$\rho_{A,N} = \frac{1}{P_N} \begin{pmatrix} 1 & \dots & 0 \\ \vdots & 0 & \vdots \\ 0 & \dots & 0 \end{pmatrix}, P_N = C$$

$$\rho_{A,0} = \frac{1}{P_N} \begin{pmatrix} 0 & \dots & 0 \\ \vdots & 0 & \vdots \\ 0 & \dots & 1 \end{pmatrix}, P_0 = C$$

$$\rho_{A,n} = \frac{1}{P_n} \begin{pmatrix} \frac{1}{N} & \cdots & \frac{1}{N} \\ \vdots & \frac{1}{N} & \vdots \\ \frac{1}{N} & \cdots & \frac{1}{N} \end{pmatrix}, P_n = N^2 C^2$$

Recall the definition of the operational (Rényi) entanglement entropy:

$$S_\alpha^{op}(\rho_A) = \sum_n P_n S(\rho_{A,n})$$

where $S_\alpha(\rho_A) = \frac{1}{1-\alpha} \log \mathrm{Tr}\,(\rho_A^\alpha)$
Expanding the sum:

$$\begin{aligned} S_\alpha^{op}(\rho_A) &= P_0 \log \mathrm{Tr}\,(\rho_{A,0}^\alpha) + \sum_{n=1}^{N-1} P_n \log \mathrm{Tr}\,(\rho_{A,n}^\alpha) + P_N \log \mathrm{Tr}\,(\rho_{A,N}^\alpha) \\ &= C \log 1 + N^2 C^2 \sum_{n=1}^{N-1} \log N(\frac{1}{N}) + C \log 1 \\ &= N^2 C^2 \sum_{n=1}^{N-1} \log 1 \\ S_\alpha^{op}(\rho_A) &= 0 \end{aligned}$$

Thus, the operational entanglement vanishes at the first order phase transition.

Analytical results have been obtained in three regimes of the tV Model, namely: $V/t \to +\infty$, $V/t \to -\infty$ and $V/t = -2$. In the next section, numerical results will be discussed.

3.3 Numerical Results

3.3.1 Operational entanglement as a function of interaction strength

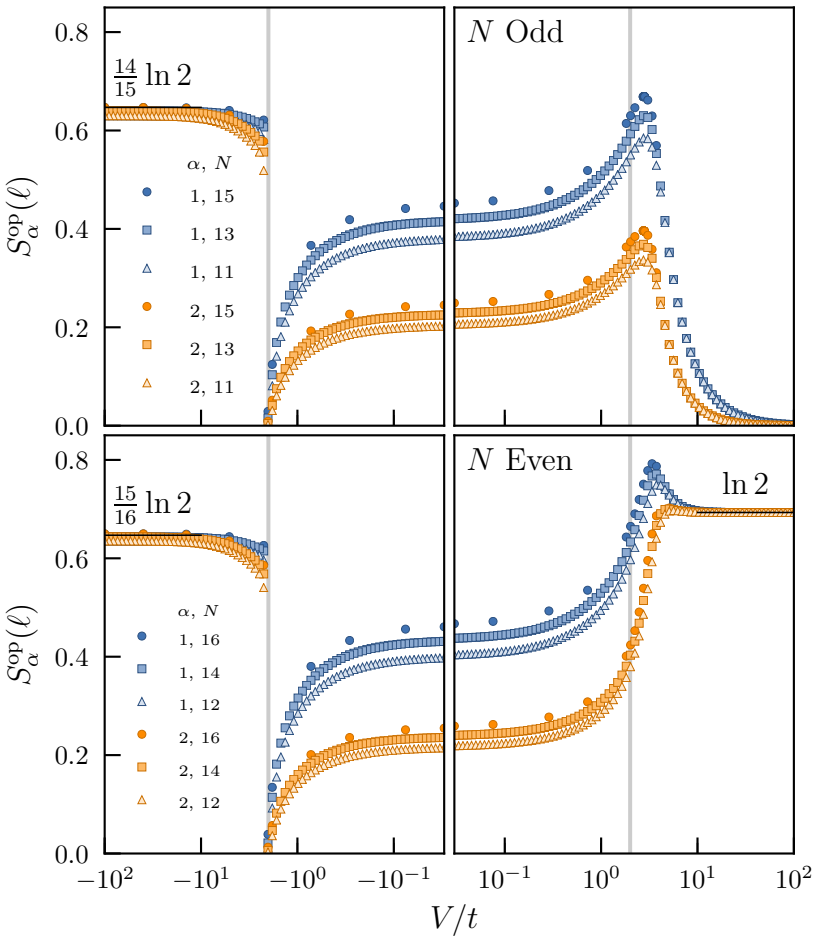

3.3.2 Scaling of operational entanglement peak

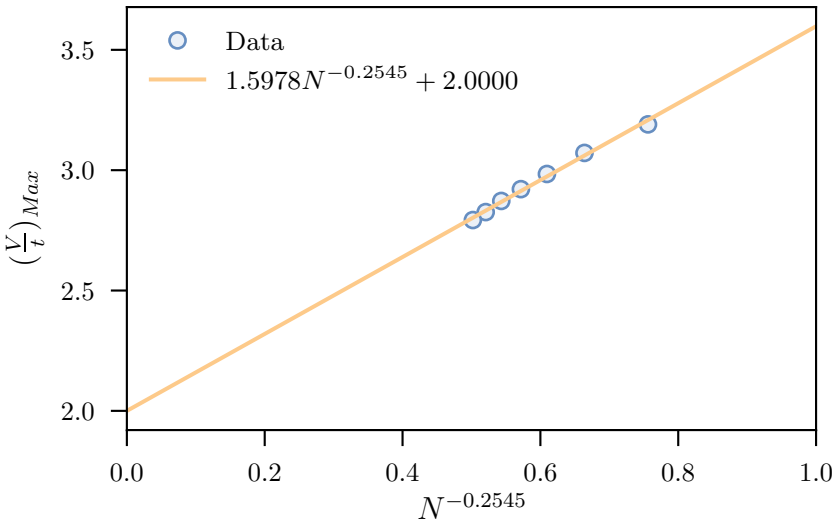

3.3.3 Entanglement of fluctuations

Appendix A

Appendix

A.1 Lanczos Algorithm

A.1.1 Introduction

The Lanczos Algorithm, takes as input a Hermitian Matrix and iteratively builds a similarity transform that makes it tridiagonal. Due to similarity, the solution of the eigenvalue problem of the tridiagonal matrix is the same as that of the original matrix. Nevertheless, some methods can exploit the tridiagonality to find the eigendecompositio more easily. In condensed matter physics, the input matrix is usually a Hamiltonian. The eigenvalues and eigenvectors of the Hamiltonian represent the energies and the associated quantum states of the system.

In the following section, the Lanczos Algorithm will be derived. Next, some methods for approximating the eigenvalues and eigenvectors will be discussed. Finally, a hopefully simple implementation of the algorithm in Python will be linked and some results will be shown.

A.1.2 Tridiagonalization of the original matrix

Let A be a Hermitian matrix of size nxn. An orthonormal transform matrix Q is needed such that:

$$T = Q^T A Q$$

where T is a tridiagonal and Hermitian matrix similar to A.

The idea is to obtain a recursive relation, starting from the known fact that T is tridiagonal and that the columns of the transform Q are mutually orthonormal. The matrix T has the form:

$$T = \begin{pmatrix} \alpha_1 & \beta_1 & & & & & 0 \\ \beta_1 & \alpha_2 & \beta_2 & & & & \\ & \beta_2 & \alpha_3 & \beta_3 & & & \\ & & \beta_3 & \ddots & \ddots & & \\ & & & \ddots & \alpha_{n-2} & \beta_{n-2} & \\ & & & & \beta_{n-2} & \alpha_{n-1} & \beta_{n-1} \\ 0 & & & & & \beta_{n-1} & \alpha_n \end{pmatrix}$$

Operating Q on both sides of the similarity relation above from the left:

$$QT = QQ^T AQ = IAQ = AQ$$

Let $\{q_1, q_2, q_3, ..., q_k\}$ be represent the mutually orthonormal columns of Q and $\{t_1, t_2, t_3, ..., t_k\}$, those of T. Then, at the k-th step of the Lanczos iteration:

$$Aq_k = Qt_k \tag{A.1}$$

$$= \begin{pmatrix} \cdots & q_{1,k-1} & q_{1,k} & q_{1,k+1} & \cdots \\ \cdots & q_{2,k-1} & q_{2,k} & q_{2,k+1} & \cdots \\ & & \vdots & & \\ \cdots & q_{n,k-1} & q_{n,k} & q_{n,k+1} & \cdots \end{pmatrix} \begin{pmatrix} \vdots \\ 0 \\ \beta_{k-1} \\ \alpha_k \\ \beta_k \\ 0 \\ \vdots \end{pmatrix} \tag{A.2}$$

The column vector only has three nonzero components. Namely, β_{k-1}, α_k and β_k. Thus, the product of this matrix-vector multiplication becomes:

$$Aq_k = \begin{pmatrix} q_{1,k-1} \\ q_{2,k-1} \\ \vdots \\ q_{n,k-1} \end{pmatrix} \beta_{k-1} + \begin{pmatrix} q_{1,k} \\ q_{2,k} \\ \vdots \\ q_{n,k} \end{pmatrix} \alpha_k + \begin{pmatrix} q_{1,k+1} \\ q_{2,k+1} \\ \vdots \\ q_{n,k+1} \end{pmatrix} \beta_k$$

Or, more compactly:

$$Aq_k = \beta_{k-1} q_{k-1} + \alpha_k q_k + \beta_k q_{k+1} \tag{A.3}$$

From this three-term recursion relation, Q can be built by finding equations for the nonzero elements of the set of columns $\{q_i\}_{i=1}^n$ (i.e the α's and β's). First, the α_k equation will be derived. Multiplying both sides of the three-term recursion relation by q_k^T from the left:

$$q_k^T Aq_k = \beta_{k-1} q_k^T q_{k-1} + \alpha_k q_k^T q_k + \beta_k q_k^T q_{k+1}$$

Since the columns of Q are mutually orthonormal, $q_k^T q_{k'} = \delta_{kk'}$. In other words, the first and third term will vanish and the second one survives. The equation for α_k is then:

$$\alpha_k = q_k^T Aq_k \tag{A.4}$$

To obtain the β_k equation, first the recursion relation is solved for $\beta_k q_{k+1}$, which gives:

$$\beta_k q_{k+1} = Aq_k - \alpha_k q_k + \beta_{k-1} q_{k-1} = (A - \alpha_k I) q_k - \beta_{k-1} q_{k-1}$$

Setting $r_k \equiv (A - \alpha_k I) q_k - \beta_{k-1} q_{k-1}$:

$$\beta_k q_{k+1} = r_k$$

Or

$$q_{k+1} = \frac{r_k}{\beta_k} \tag{A.5}$$

where $\beta_k \neq 0$ and, since q_{k+1} is an orthonormal vector, $\beta_k = ||r_k||_2$, such that q_{k+1} is normalized.

Note that the α_k and β_k terms of the three-term recursion relation have been accounted for. As for the β_{k-1}, a "bottom rung" for the recursion has to be set. The tridiagonal matrix T does not have a β_{k-1} term. Thus, for $k = 1$, the $\beta_{k-1}q_{k-1}$ term is set to $\beta_0 q_0 = 0$. Now the columns of Q can be built by iterating from $k = 1$ to $k = n$.

A.1.3 Algorithm

1. Set $r_0 = q_1$,$\beta_0 = 1$ and $q_0 = 0$
2. For k=1,2,3,...,n:
3. $q_{k+1} = \frac{r_k}{\beta_k}$
4. $\alpha_k = q_k^T A q_k$
5. $r_k = (A - \alpha_k I)q_k - \beta_{k-1}q_{k-1}$
6. $\beta_k = ||r_k||_2$
7. Reorthonormalize $\{q_i\}_{i=1}^k$ if necessary
8. Approximate Eigenvalues and Eigenvectors (Can be done after the loop instead)

Line 1: β_0 is set to 1 since it is the norm of r_0 and $r_0 = q_1$, where q_1 is a normalized vector.

Line 2: The for loop runs from $k = 1$ all the way up to $k = n$, where n is the total number of columns. Depending of the eigenvalues desired, this loop can instead be a while loop that ends whenever the eigenvalues have reached a desired tolerance.

Line 7: Due to finite precision errors, the set of supposedly mutually orthonormal vectors $\{q_i\}_{i=1}^k$ will actually lose their orthonormality at later Lanczos steps. When this happens, a reorthonormalization scheme, such as the Grahm-Schmidt Process, has to be employed.

Line 8: Again, depending on the problem and the desired eigenpairs, the approximation can be done for the current version of the tridiagonal matrix at step k, call it T_k. Alternatively, it could be done after the for loop has finished and the full tridiagonal matrix has been T built. There is no strict requirement on which iterative method should be used to find the eigendecomposition (QR Method, Power Iteration, Inverse Power Iteration, etc...).

A.1.4 Code

An implementation of the Lanczos Algorithm in Python can be found in: https://github.com/ecasian
The code generates a random, sparse, hermitian matrix of specified size, finds a tridiagonal representation via Lanczos and calculates the full eigendecomposition via QR Algorithm or finds the smallest eigenvalue via Inverse Power Iteration. A blackbox

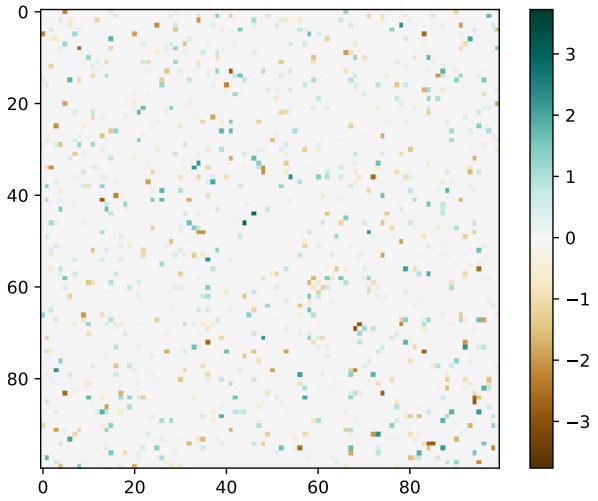

Figure A.1: INSERT CAPTION.

function, part of the numpy.linalg package, numpy.linalg.eigsh(), solves the eigenvalue problem for the input matrix so a comparison can be made with the code results.

A.1.5 Results

The following colormap represents a sparse and hermitian matrix of dimensions nxn that was fed to the linked Lanczos code.

The Lanczos iterations were carried from $k = 1$ to $k = n = 100$. First, Lanczos was ran without reorthonormalizing the columns of the transform matrix Q.

Observe how the matrix starts to look tridiagonal, but has some large nonzero entries far away from the diagonal. This is the result of finite precision error. Via the Grahm-Schmidt Procedure, a full reorthonormalization was then done at each Lanczos step. The colormap below shows the result.

Barring some small nonzero entries in the bottom right, most likely due also to finite precision, the matrix was now tridiagonalized successfully.

The following scatter plot shows the eigenvalues obtained using the Lanczos code linked and those obtained using numpy.linalg.eigsh(). These eigenvalues correspond to the same matrix generated for the plots in the previous section.

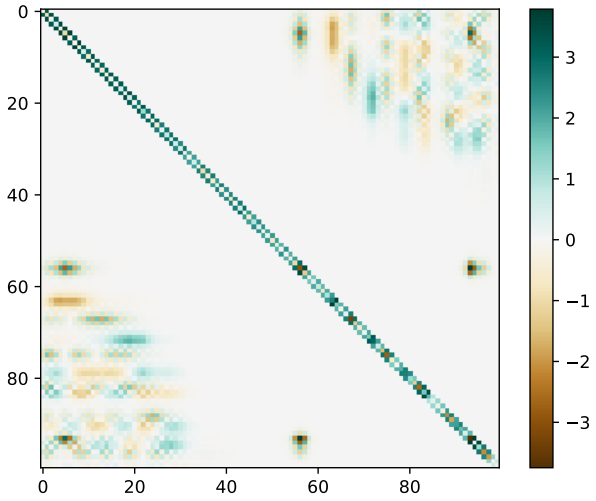

Figure A.2: INSERT CAPTION.

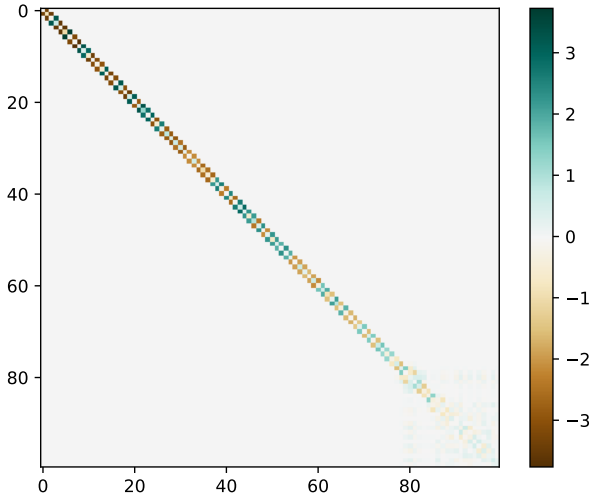

Figure A.3: INSERT CAPTION.

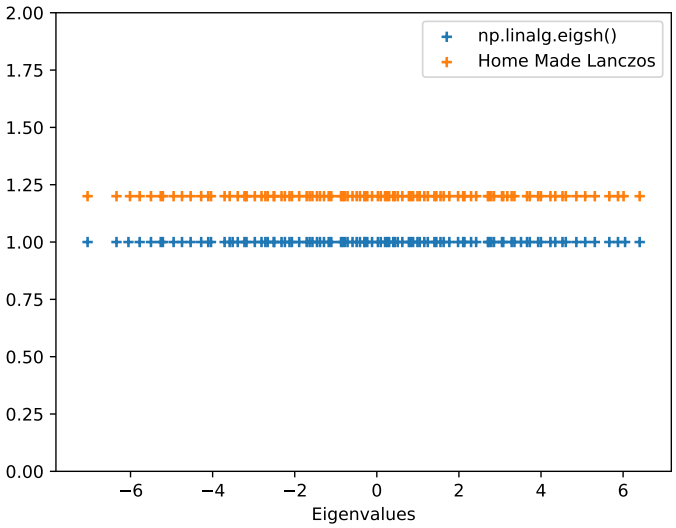

Figure A.4: INSERT CAPTION.

Appendix B

Appendix

B.1 Evaluating the n-particle partition entanglement

In this appendix, we show that the n-RDM of spinless hardcore particles on a lattice can be written as a tensor product of two lower-rank matrices. This simplification significantly reduces the numerical cost for calculating n-RDM for such quantum systems.

In general, for a pure quantum state $|\Psi\rangle$ in some Hilbert space $\mathcal{H}$ that can be written as the tensor product space $A \otimes B$, we can write

$$|\Psi\rangle = \sum_{i,j} C_{i,j} |\psi_i^A\rangle |\psi_j^B\rangle, \tag{B.1}$$

where $\{|\psi_i^A\rangle\}$ and $\{|\psi_j^B\rangle\}$ are orthonormal bases in the two Hilbert spaces A and B, respectively. Accordingly, the system degrees of freedom are bipartitioned between the two subsets $\{|\psi_i^A\rangle\}$ and $\{|\psi_j^B\rangle\}$. Using the product basis $\{|\psi_i^A\rangle|\psi_j^B\rangle\}$, the full density matrix can be written as

$$\rho = |\Psi\rangle\langle\Psi| = \sum_{i,j,i',j'} |\psi_i^A\rangle|\psi_j^B\rangle C_{i,j} C^*_{i',j'} \langle\psi_{i'}^A|\langle\psi_{j'}^B|. \tag{B.2}$$

The reduced density matrix ρ_A (ρ_B) of subspace A (B) , is obtained from ρ by tracing out the degrees of freedom of subspace B (A),

$$\rho_A = \sum_m \langle\psi_m^B|\rho|\psi_m^B\rangle = \sum_{i,j} |\psi_i^A\rangle \left(\sum_m C_{i,m} C^*_{j,m} \right) \langle\psi_j^A|, \tag{B.3}$$

$$\rho_B = \sum_m \langle\psi_m^A|\rho|\psi_m^A\rangle = \sum_{i,j} |\psi_i^B\rangle \left(\sum_m C_{m,i} C^*_{m,j} \right) \langle\psi_j^B|. \tag{B.4}$$

Moreover, the reduced density matrices can be generated using the linear maps $G_{AB} : S_B \to S_A$ as $\rho_A = G_{AB} G_{AB}^\dagger$ and $\rho_B = (G_{AB}^\dagger G_{AB})^T$ where

$$G_{AB} = \sum_{i,j} C_{i,j} |\psi_i^A\rangle\langle\psi_j^B|. \tag{B.5}$$

Note that, in general, the matrix representing the linear maps G_{AB} is rectangular since the dimensions of the Hilbert spaces A and B can differ.

B.1.1 Particle bipartition

Let us now consider a quantum system of N spinless hardcore particles in a state $|\Psi\rangle = \sum_i \chi_i |\psi_i^N\rangle$, where $\{|\psi_i^N\rangle\}$ are the N particle second-quantization basis states, where each basis state corresponds to a single, possible, occupation number configuration (ONC). Now we recall that each ONC state is a linear combination of the distinguished particles states $\{|\psi_{i,j}^N\rangle\}$ as $|\psi_i^N\rangle = \sum_j \frac{f_j}{\sqrt{N!}} |\psi_{i,j}^N\rangle$, where j runs over all possible particle permutations (PPs) and $f_j = e^{-i\phi_j}$ is the corresponding phase factor. Accordingly, we can write

$$|\Psi\rangle = \sum_{i,j} \frac{\chi_i f_j}{\sqrt{N!}} |\psi_{i,j}^N\rangle. \tag{B.6}$$

Now we partition N into two sets of particles: n_A and the remainder $n_B = N - n_A$. The distinguished particles basis $\{|\psi_{i,j}^N\rangle\}$ can be written as a tensor product of the two partitions basis

$$|\psi_{i,j}^N\rangle = |\psi_{i_A,j_A}^{n_A}\rangle |\psi_{i_B,j_B}^{n_B}\rangle, \tag{B.7}$$

where each ONC (labelled by i) of the N particles corresponds to a unique pair of ONCs i_A and i_B of the n_A and n_B particles, respectively. Similarly, each PP j of the N particles corresponds to a unique pair of PPs: j_A and j_B of the n_A and n_B particles.

$$|\Psi\rangle = \sum_{i_A,i_B,j_A,j_B} C_{i_A,i_B,j_A,j_B} |\psi_{i_A,j_A}^{n_A}\rangle |\psi_{i_B,j_B}^{n_B}\rangle, \tag{B.8}$$

with

$$C_{i_A,i_B,j_A,j_B} = \frac{\chi_i f_j}{\sqrt{N!}}. \tag{B.9}$$

The C_{i_A,i_B,j_A,j_B} depends on the indices i and j through the multiplication of χ_i and f_j, and without loss of generality, we can take

$$C_{i_A,i_B,j_A,j_B} = \tilde{C}_{i_A,i_B} \Phi_{j_A,j_B}. \tag{B.10}$$

Moreover, the dependence of Φ_{j_A,j_B} on the PP indices only guarantees that $|\Phi_{j_A,j_B}|^2 = \textit{constant}$ that can be absorbed in $\tilde{C}_{i_A,i_B}$. Thus, we can set $|\Phi_{j_A,j_B}|^2 = 1$. Based on the fact that applying a particle permutation two one group of particles results in an overall phase factor that does not depend on the permutation of the other group of particles, we write

$$\Phi_{j_A,j_B} = F_{j_A}^{(A)} F_{j_B}^{(B)}, \tag{B.11}$$

with $|F_{j_A}^{(A)}|^2 = |F_{j_B}^{(B)}|^2 = 1$. Substituting in Eq. (B.8) we find

$$|\Psi\rangle = \sum_{i_A,i_B,j_A,j_B} \tilde{C}_{i_A,i_B} F_{j_A}^{(A)} F_{j_B}^{(B)} |\psi_{i_A,j_A}^{n_A}\rangle |\psi_{i_B,j_B}^{n_B}\rangle, \tag{B.12}$$

Let us now calculate the reduced density matrix of ρ_A using

$$G_{n_A n_B} = \sum_{i_A,i_B,j_A,j_B} \tilde{C}_{i_A,i_B} F_{j_A}^{(A)} F_{j_B}^{(B)} |\psi_{i_A,j_A}^{n_A}\rangle \langle \psi_{i_B,j_B}^{n_B}|, \tag{B.13}$$

as

$$\rho_A = G_{n_A n_B} G^{\dagger}_{n_A n_B} \tag{B.14}$$

$$= \sum_{i_A, j_A, i'_A, j'_A} |\psi^{n_A}_{i_A, j_A}\rangle \sum_{i_B} \left(\tilde{C}_{i_A, i_B} \tilde{C}^{*}_{i'_A, i_B} \right) F^{(A)}_{j_A} F^{*(A)}_{j'_A} \sum_{j_B} \left| F^{(B)}_{j_B} \right|^2 \langle \psi^{n_A}_{i'_A, j'_A}|$$

$$= n_B! \sum_{i_A, j_A, i'_A, j'_A} |\psi^{n_A}_{i_A, j_A}\rangle D_{i_A, i'_A} \Phi_{j_A, j'_A} \langle \psi^{n_A}_{i'_A, j'_A}|, \tag{B.15}$$

with $D_{i_A, i'_A} = \sum_{i_B} \tilde{C}_{i_A, i_B} \tilde{C}^{*}_{i'_A, i_B}$ and $\Phi_{j_A, j'_A} = F^{(A)}_{j_A} F^{*(A)}_{j'_A}$. From Eq. (B.15) we see that ρ_A is a Kronecker product (tensor product) of the lower-rank Hermitian matrices D and Φ. where D can be calculated considering a single PP for each particle partition and the elements of Φ are the product of the relative phases of the chosen partitions (B.11)

B.1.2 Eigenvalues

Let V_D and V_Φ be two unitary transformations that diagonalize the sub matrices D and Φ, respectively. Such that $V_D^{\dagger} D V_D = \Lambda$ and $V_\Phi^{\dagger} \Phi V_\Phi = W$, where Λ and W are diagonal matrices with eigenvalues $\{\lambda_k\}$ and $\{w_l\}$. If we construct the unitary transformation U as

$$U = V_D \otimes V_\Phi, \tag{B.16}$$

and calculate $U^{\dagger}(\rho_A / n_B!)U$ we find

$$U^{\dagger} \left(\frac{\rho_A}{n_B!} \right) U = \sum_{k,l} |\psi^{n_1}_{k,l}\rangle \lambda_k w_l \langle \psi^{n_1}_{k,l}|. \tag{B.17}$$

Accordingly, the unitary transformation U diagonalizes ρ_A and the eigenvalues of ρ_A are $n_B! \lambda_k w_l$. Moreover, Φ has the structure of a simple projection operator onto the non-normalized state $|F^{(A)}\rangle = \sum_j^{n_A!} F^{(A)}_j |j\rangle = \sum_j^{n_A!} e^{i\phi_j} |j\rangle$ as $\Phi = |F^{(A)}\rangle\langle F^{(A)}|$. The only eigenstate of Φ with a nonzero eigenvalue is $|F^{(A)}\rangle$, where $\Phi |F^{(A)}\rangle = |F^{(A)}\rangle \langle F^{(A)}|F^{(A)}\rangle = n_A! |F^{(A)}\rangle$.

Therefore, we conclude that the nonzero eigenvalues of ρ_A are $n_A! n_B! \lambda_k$, where λ_k are the eigenvalues of the matrix D that is constructed using only one PP of each of the sets $\{|\psi^{n_A}_{i_A, j_A}\rangle\}$ and $\{|\psi^{n_B}_{i_B, j_B}\rangle\}$. As the rank of D is smaller than that of the n-RDM by a factor of $n_A! n_B!$ the numerical effort involved in calculating the eigenvalues of the n-RDM is enormously reduced.

B.2 n-particle partition entanglement in the $V/t \to \infty$ limit

Here we calculate the n-particle partition entanglement of the one-dimensional fermionic $t - V$ model at half filling ($N = M/2$) in the infinite repulsion limit ($V/t \to \infty$). In this limit, the Hamiltonian of the model (Eq. (2.18)) is reduced to

$$H = V \sum_i n_i n_{i+1} \tag{B.18}$$

which is diagonal in the occupation number representation with a two-fold degenerate ground state, where, at half filling, the fermions can avoid having any nearest neighbors by occupying sites with only odd indices ($|\psi_{\text{odd}}\rangle = |1010\cdots10\rangle$) or only even indices ($|\psi_{\text{even}}\rangle = |0101\cdots01\rangle$). Thus, one can write the ground state in this limit, as a superposition of $|\psi_{\text{odd}}\rangle$ and $|\psi_{\text{even}}\rangle$:

$$|\Psi\rangle = \cos(\Theta)e^{i\delta}|\psi_{\text{odd}}\rangle + \sin(\Theta)|\psi_{\text{even}}\rangle, \tag{B.19}$$

where we parametrize the amplitudes and the relative phase of the odd/even states using Θ and δ. Note that for $\delta = 0$ and $\Theta = \pi/4$ ($\Theta = 3\pi/4$), the ground state $|\Psi\rangle$ is also an eigenstate of the inversion operator P (Eq. (2.22)) with eigenvalue ±1 where

$$P|\Phi_\pm\rangle = \pm|\Phi_\pm\rangle = \pm\left(\frac{1}{\sqrt{2}}|\psi_{\text{odd}}\rangle \pm \frac{1}{\sqrt{2}}|\psi_{\text{even}}\rangle\right). \tag{B.20}$$

The degeneracy persists in the case of finite interaction V/t for even/odd N with PBC/APBC. The degeneracy is lifted for odd/even N with APBC/PBC with the resulting ground state in the infinite repulsion limit approaching an eigenstate of P:

$$|\Psi\rangle = |\Phi_+\rangle = \frac{1}{\sqrt{2}}|\psi_{\text{odd}}\rangle + \frac{1}{\sqrt{2}}|\psi_{\text{even}}\rangle. \tag{B.21}$$

We now consider the n-particle partition entanglement of the degenerate ground state $|\Psi\rangle$ defined in Eq. (B.19), where we can write the corresponding full density matrix ρ as

$$\begin{aligned}\rho \quad &= \cos^2(\Theta)|\psi_{\text{odd}}\rangle\langle\psi_{\text{odd}}| + \sin^2(\Theta)|\psi_{\text{even}}\rangle\langle\psi_{\text{even}}| \\ &+ \sin(\Theta)\cos(\Theta)e^{i\delta}|\psi_{\text{odd}}\rangle\langle\psi_{\text{even}}| + \sin(\Theta)\cos(\Theta)e^{-i\delta}|\psi_{\text{even}}\rangle\langle\psi_{\text{odd}}|,\end{aligned} \tag{B.22}$$

If we partition the N particles into two distinguishable sets of $n_A = n$ and $n_B = N-n$ particles, we can write the states $|\psi_{odd}\rangle$ and $|\psi_{even}\rangle$ in terms of the first-quantized basis states of the two partitions as

$$|\psi_{\text{odd}}\rangle = \sum_{i_A,i_B,j_A,j_B} \frac{f^{\text{odd}}_{i_A,i_B,j_A,j_B}}{\sqrt{N!}}|\psi^{n_A,\text{odd}}_{i_A,j_A}\rangle|\psi^{n_B,\text{odd}}_{i_B,j_B}\rangle, \tag{B.23}$$

$$|\psi_{\text{even}}\rangle = \sum_{i_A,i_B,j_A,j_B} \frac{f^{\text{even}}_{i_A,i_B,j_A,j_B}}{\sqrt{N!}}|\psi^{n_A,\text{even}}_{i_A,j_A}\rangle|\psi^{n_B,\text{even}}_{i_B,j_B}\rangle, \tag{B.24}$$

where the indices i_A and i_B label possible occupation number configurations (ONCs) in both partitions A and B while j_A and j_B label different particle permutations (PPs). Also, $f^{\text{odd}}_{i_A,i_B,j_A,j_B}$ and $f^{\text{even}}_{i_A,i_B,j_A,j_B}$ are overall phase factors, where the superscript odd (even) is to indicate that only sites with odd (even) indices are occupied. We note that in this decomposition the states $|\psi_{\text{even}}\rangle$ and $|\psi_{\text{odd}}\rangle$ are constructed from non-overlapping subspaces (even/odd) of partition B. Similarly for partition A. By tracing out all degrees of freedom in B from ρ (Eq. (B.22)), we can write the reduced density matrix ρ_A as

$$\rho_A = \text{Tr}_B\,\rho = \cos^2(\Theta)\text{Tr}_B\,|\psi_{\text{odd}}\rangle\langle\psi_{\text{odd}}| + \sin^2(\Theta)\text{Tr}_B\,|\psi_{\text{even}}\rangle\langle\psi_{\text{even}}|, \tag{B.25}$$

where the trace of the mixed terms ($|\psi_{\text{odd}}\rangle\langle\psi_{\text{even}}|$, $|\psi_{\text{even}}\rangle\langle\psi_{\text{odd}}|$) vanishes due to the non-sharing of B basis states. Moreover, $\rho^{\text{odd}}_A = \text{Tr}_B\,|\psi_{\text{odd}}\rangle\langle\psi_{\text{odd}}|$ and $\rho^{\text{even}}_A =$

$\mathrm{Tr}_B\,|\psi_{\mathrm{even}}\rangle\langle\psi_{\mathrm{even}}|$ contribute separately to the spectrum of ρ_A due to the non-sharing of A basis states.

We now calculate the spectrum of ρ_A^{odd}. Note that the state $|\psi_{\mathrm{odd}}\rangle$ represents a single ONC of the N particles and as a result the ONC i_A is uniquely determined by i_B in the product states $|\psi_{i_A,j_A}^{n_A,\mathrm{odd}}\rangle|\psi_{i_B,j_B}^{n_B,\mathrm{odd}}\rangle$. Therefore, ρ_A^{odd} does not connect any pair of states, in the set $\{|\psi_{i_A,j_A}^{n_A,\mathrm{odd}}\rangle\}$, with different ONC i_A. This result, combined with the formalism presented in **??**, allows us to identify that the sector of ρ_A^{odd} that connects states in $\{|\psi_{i_A,j_A}^{n_A,\mathrm{odd}}\rangle\}$ with fixed PP j_A is diagonal with $\binom{N}{n}$ equal non-zero elements of value $\frac{1}{N!}$. $\binom{N}{n}$ is the number of possible ONCs in the partition A with $n_A = n$ and we only consider the contribution of a single PP j_B to $\mathrm{Tr}_B\,|\psi_{\mathrm{odd}}\rangle\langle\psi_{\mathrm{odd}}|$. It then follows from **??** that the non-zero eigenvalues of ρ_A^{odd} can be obtained by rescaling the above eigenvalues by a factor of $n_A!n_B! = n!(N-n)!$. By an equivalent set of arguments ρ_A^{even} has the same eigenvalues. Combining all the above and using Eq. (B.25), we find that ρ_A has two sets of eigenvalues: $\binom{N}{n}$ eigenvalues of $\cos^2(\Theta)/\binom{N}{n}$ and $\binom{N}{n}$ eigenvalues of $\sin^2(\Theta)/\binom{N}{n}$. Therefore, the Rényi entanglement entropies are

$$S_\alpha(n) = \ln\binom{N}{n} + \frac{1}{1-\alpha}\ln\left[\cos^{2\alpha}(\Theta) + \sin^{2\alpha}(\Theta)\right], \tag{B.26}$$

and the von Neumann entropy ($\alpha = 1$) is

$$S_1(n) = \ln\binom{N}{n} - \cos^2(\Theta)\ln\left[\cos^2(\Theta)\right] - \sin^2(\Theta)\ln\left[\sin^2(\Theta)\right]. \tag{B.27}$$

According to Eqs. (B.26) and (B.27), the maximum entropy corresponds to $\Theta = \pi/4$ and $3\pi/4$ ($|\Psi\rangle = \frac{e^{i\delta}}{\sqrt{2}}|\psi_{\mathrm{odd}}\rangle + \frac{1}{\sqrt{2}}|\psi_{\mathrm{even}}\rangle$), where all the $2\binom{N}{n}$ eigenvalues of ρ_A are equal and thus all the Rényi entropies are equal to

$$S_\alpha(n) = \ln\binom{N}{n} + \ln 2. \tag{B.28}$$

For $\Theta = 0$ and $\pi/2$, $|\Psi\rangle = |\psi_{\mathrm{odd}}\rangle$ or $|\psi_{\mathrm{even}}\rangle$, only $\binom{N}{n}$ equal eigenvalues survive yielding a minimum entropy of

$$S_\alpha(n) = \ln\binom{N}{n}. \tag{B.29}$$

These limits can be seen in Fig. 2.6 for $V/t \gg 1$.

Bibliography

[rep,] Barghathi, H and Casiano-Diaz, E and Del Maestro, A, 2017 GitHub Repository, `https://github.com/DelMaestroGroup/PartEntFermions` .

[cod,] Melko, R G and Iouchtchenko D, 2016, GitHub Repository, `https://github.com/MelkoCollective/BH_diagonalize`.

[Balachandran et al., 2013] Balachandran, A. P., Govindarajan, T. R., de Queiroz, A. R., and Reyes-Lega, A. F. (2013). Entanglement and Particle Identity: A Unifying Approach. *Phys. Rev. Lett.*, 110(8):080503.

[Barnum et al., 2004] Barnum, H., Knill, E., Ortiz, G., Somma, R., and Viola, L. (2004). A Subsystem-Independent Generalization of Entanglement. *Phys. Rev. Lett.*, 92(10):107902.

[Benatti et al., 2012] Benatti, F., Floreanini, R., and Marzolino, U. (2012). Entanglement robustness and geometry in systems of identical particles. *Phys. Rev. A*, 85(4):042329.

[Calabrese and Cardy, 2004] Calabrese, P. and Cardy, J. (2004). Entanglement entropy and quantum field theory. *J. Stat. Mech.: Theor. Exp.*, 2004(06):P06002.

[Calabrese et al., 2011a] Calabrese, P., Mintchev, M., and Vicari, E. (2011a). Entanglement Entropy of One-Dimensional Gases. *Phys. Rev. Lett.*, 107(2).

[Calabrese et al., 2011b] Calabrese, P., Mintchev, M., and Vicari, E. (2011b). The entanglement entropy of one-dimensional systems in continuous and homogeneous space. *J. Stat. Mech. Theor. Exp.*, 2011(09):P09028.

[Cazalilla, 2004] Cazalilla, M. A. (2004). Bosonizing one-dimensional cold atomic gases. *J. Phys. B: At. Mol. Opt. Phys.*, 37(7):S1.

[Cloizeaux, 1966] Cloizeaux, J. D. (1966). A soluble fermi-gas model. validity of transformations of the bogoliubov type. *J. Math. Phys.*, 7(12):2136–2144.

[Cloizeaux and Gaudin, 1966] Cloizeaux, J. D. and Gaudin, M. (1966). Anisotropic linear magnetic chain. *J. Math. Phys.*, 7(8):1384–1400.

[Dalton et al., 2017] Dalton, B. J., Goold, J., Garraway, B. M., and Reid, M. D. (2017). Quantum entanglement for systems of identical bosons: I. general features. *Phys. Scrip.*, 92(2):023004.

[Ding and Yang, 2009] Ding, W. and Yang, K. (2009). Entanglement entropy and mutual information in Bose-Einstein condensates. *Phys. Rev. A*, 80(1):012329.

[Drut and Porter, 2015] Drut, J. E. and Porter, W. J. (2015). Hybrid Monte Carlo approach to the entanglement entropy of interacting fermions. *Phys. Rev. B*, 92(12):125126.

[Drut and Porter, 2016] Drut, J. E. and Porter, W. J. (2016). Entanglement, noise, and the cumulant expansion. *Phys. Rev. E*, 93(4):043301.

[Dunningham et al., 2005] Dunningham, J., Rau, A., and Burnett, K. (2005). From Pedigree Cats to Fluffy-Bunnies. *Science*, 307(5711):872.

[Dzyaloshinskii and Larkin, 1974] Dzyaloshinskii, I. E. and Larkin, A. I. (1974). Correlation functions for a one-dimensional Fermi system with long-range interaction (Tomonaga model). *Sov. Phys. JETP*, 38:202.

[Ghirardi and Marinatto, 2004] Ghirardi, G. and Marinatto, L. (2004). General criterion for the entanglement of two indistinguishable particles. *Phys. Rev. A*, 70(1):012109.

[Giamarchi, 2004] Giamarchi, T. (2004). *Quantum Physics in One Dimension*. Oxford University Press, Oxford, U.K.

[Grover, 2013] Grover, T. (2013). Entanglement of Interacting Fermions in Quantum Monte Carlo Calculations. *Phys. Rev. Lett.*, 111(13):130402.

[Haldane, 1981] Haldane, F. D. M. (1981). Effective Harmonic-Fluid Approach to Low-Energy Properties of One-Dimensional Quantum Fluids. *Phys. Rev. Lett.*, 47(25):1840.

[Haque et al., 2007] Haque, M., Zozulya, O., and Schoutens, K. (2007). Entanglement Entropy in Fermionic Laughlin States. *Phys. Rev. Lett.*, 98(6):060401.

[Haque et al., 2009] Haque, M., Zozulya, O. S., and Schoutens, K. (2009). Entanglement between particle partitions in itinerant many-particle states. *J. Phys. A: Math. Theor.*, 42(50):504012.

[Hastings et al., 2010] Hastings, M. B., González, I., Kallin, A. B., and Melko, R. G. (2010). Measuring Renyi Entanglement Entropy in Quantum Monte Carlo Simulations. *Phys. Rev. Lett.*, 104(15):157201.

[Herdman and Del Maestro, 2015] Herdman, C. M. and Del Maestro, A. (2015). Particle partition entanglement of bosonic Luttinger liquids. *Phys. Rev. B*, 91(18):184507.

[Herdman et al., 2014] Herdman, C. M., Roy, P. N., Melko, R. G., and Del Maestro, A. (2014). Particle entanglement in continuum many-body systems via quantum Monte Carlo. *Phys. Rev. B*, 89(14):140501.

[Islam et al., 2015] Islam, R., Ma, R., Preiss, P. M., Tai, M. E., Lukin, A., Rispoli, M., and Greiner, M. (2015). Measuring entanglement entropy in a quantum many-body system. *Nature*, 528(7580):77.

[Jordan and Wigner, 1928] Jordan, P. and Wigner, E. (1928). Über das paulische äquivalenzverbot. *Zeitschrift für Physik*, 47(9):631.

[Kampf et al., 2003] Kampf, A. P., Sekania, M., Japaridze, G. I., and Brune, P. (2003). Nature of the insulating phases in the half-filled ionic hubbard model. *J. Phys. Condens. Matter*, 15(34):5895.

[Katsura and Hatsuda, 2007] Katsura, H. and Hatsuda, Y. (2007). Entanglement entropy in the Calogero-Sutherland model. *J. Phys. A: Math. Theor.*, 40(46):13931.

[Killoran et al., 2014] Killoran, N., Cramer, M., and Plenio, M. B. (2014). Extracting entanglement from identical particles. *Phys. Rev. Lett.*, 112:150501.

[Liu and Fan, 2010] Liu, Z. and Fan, H. (2010). Particle entanglement in rotating gases. *Phys. Rev. A*, 81:062302.

[McMinis and Tubman, 2013] McMinis, J. and Tubman, N. M. (2013). Renyi entropy of the interacting Fermi liquid. *Phys. Rev. B*, 87:081108.

[Melko et al., 2016] Melko, R. G., Herdman, C. M., Iouchtchenko, D., Roy, P. N., and Del Maestro, A. (2016). Entangling qubit registers via many-body states of ultracold atoms. *Phys. Rev. A*, 93(4):042336.

[Porter and Drut, 2016] Porter, W. J. and Drut, J. E. (2016). Entanglement spectrum and Rényi entropies of nonrelativistic conformal fermions. *Phys. Rev. B*, 94(16):165112.

[Santachiara et al., 2007] Santachiara, R., Stauffer, F., and Cabra, D. C. (2007). Entanglement properties and momentum distributions of hard-core anyons on a ring. *J. Stat. Mech.: Theor. Exp.*, 2007(05):L05003.

[Schliemann et al., 2001] Schliemann, J., Cirac, J. I., Kuś, M., Lewenstein, M., and Loss, D. (2001). Quantum correlations in two-fermion systems. *Phys. Rev. A*, 64(2):022303.

[Shi, 2003] Shi, Y. (2003). Quantum entanglement of identical particles. *Phys. Rev. A*, 67(2):024301.

[Shi, 2004] Shi, Y. (2004). Quantum entanglement in second-quantized condensed matter systems. *J. Phys. A: Math. Gen*, 37(26):6807.

[Simon, 2002] Simon, C. (2002). Natural entanglement in Bose-Einstein condensates. *Phys. Rev. A*, 66(5):052323.

[Tichy et al., 2011] Tichy, M. C., Mintert, F., and Buchleitner, A. (2011). Essential entanglement for atomic and molecular physics. *J. Phys. B: Atom., Mol. and Opt. Phys.*, 44(19):192001.

[Tomonaga, 1951] Tomonaga, S.-I. (1951). Remarks on Bloch's Method of Sound Waves applied to Many-Fermion Problems. *Prog. Theor. Phys.*, 5(4):544.

[Wiseman et al., 2003] Wiseman, H. M., Bartlett, S. D., and Vaccaro, J. A. (2003). Ferreting out the Fluffy Bunnies: Entanglement constrained by Generalized superselection rules. *arXiv*.

[Wiseman and Vaccaro, 2003a] Wiseman, H. M. and Vaccaro, J. A. (2003a). Entanglement of Indistinguishable Particles Shared between Two Parties. *Phys. Rev. Lett.*, 91:097902.

[Wiseman and Vaccaro, 2003b] Wiseman, H. M. and Vaccaro, J. A. (2003b). Entanglement of indistinguishable particles shared between two parties. *Phys. Rev. Lett.*, 91:097902.

[Zanardi, 2001] Zanardi, P. (2001). Virtual Quantum Subsystems. *Phys. Rev. Lett.*, 87(7):077901.

[Zanardi, 2002] Zanardi, P. (2002). Quantum entanglement in fermionic lattices. *Phys. Rev. A*, 65(4):042101.

[Zanardi and Wang, 2002] Zanardi, P. and Wang, X. (2002). Fermionic entanglement in itinerant systems. *J. Phys. A: Math. and Gen.*, 35(37):7947.

[Zozulya et al., 2008] Zozulya, O., Haque, M., and Schoutens, K. (2008). Particle partitioning entanglement in itinerant many-particle systems. *Phys. Rev. A*, 78(4):042326.

[Zozulya et al., 2007] Zozulya, O. S., Haque, M., Schoutens, K., and Rezayi, E. H. (2007). Bipartite entanglement entropy in fractional quantum Hall states. *Phys. Rev. B*, 76(12):125310.